UNIVERSITY OF OTTAWA

CHEMICAL AND BIOLOGICAL ENGINEERING DEPARTMENT

THERMAL ENERGY STORAGE IN ADSORBENT BEDS

By: Burcu Ugur

A thesis submitted to the Faculty of Graduate and Postdoctoral Studies

in partial fulfillment of the requirements for the degree of

MASTER OF APPLIED SCIENCE

Summer, 2013

ABSTRACT

Total produced energy in the world is mostly consumed as thermal energy which is used for space or water heating. Currently, more than 85% of total thermal energy consumption is supplied from fossil fuels. This high consumption rate increases the depletion risk of fossil fuels as well as causing a tremendous release of hazardous gases such as carbon dioxide, carbon monoxide, sulfur oxides, nitrogen oxides and particulate matter that effects both environment and human health. Those drawbacks force humankind to search for new technologies, like renewables, to reduce fossil fuel dependency on thermal energy production.

Thermal energy storage in adsorbent beds is one of the resulting technologies. Adsorption is an exothermic process in which a fluid (adsorbate) diffuses into the pores of a porous solid material (adsorbent) and trapped into the crystal lattice. In this system, exothermic adsorption of water vapor from air is carried out by using hybrid adsorbent of activated alumina and zeolite. In previous studies, through literature review, this adsorbent was selected to be the most efficient adsorbent for this process due to its high water adsorption capacity, high heat of adsorption, and stability [Dicaire and Tezel, 2011]. In this study, previous studies started on this project was confirmed and pursued by trying to increase the efficiency of the process and confirm the feasibility and applicability of this system in larger scales.

In this thesis, various zeolite and activated alumina hybrid adsorbents with varying zeolite compositions were screened to find the most efficient adsorbent for thermal energy

storage process that gives the highest energy density. Then, existing small column was replaced with a new one, which is 16 times bigger in volume, in order to confirm the feasibility of this process at larger scales. Applicability of on-off heat release in adsorption process was also investigated by conducting several on-off experiments at different on-off time periods. Moreover, exothermic adsorption process was modeled by doing mass and energy balances in the column, water accumulation balance in the pellets, and energy balance in the column wall. Validity of this model was confirmed by comparing it with experimental results at different column volumes, and at different volumetric flow rates. Finally, an overall plant design, capital cost and thermal energy price estimations were done for adsorption thermal energy storage plants for different storage capacities and payback periods.

RÉSUMÉ

La plupart de l'énergie produite dans le monde est utilisée sous forme d'énergie thermique pour le chauffage des édifices et le chauffage de l'eau. En ce moment, plus que 85% de l'énergie thermique vient des combustibles fossiles. Cette consommation augmente le risque d`épuisement des combustibles fossiles et produit aussi des gaz dangereux pour l`environnement et la santé humaine, tel que le dioxyde de carbone, le monoxyde de carbone, les oxydes de soufre, les oxydes d`azote et la matière particulaire. Ces désavantages obligent l`humanité de chercher pour de nouvelles technologies afin de réduire la dépendance de la production d`énergie thermique aux combustibles fossiles.

Un lit d`adsorbant pour l`entreposage de l`énergie thermique est l`une des technologies qui peut être utilisée. L`adsorption est un processus exothermique dans lequel certaines molécules d'un fluide diffuse dans les pores d`un solide poreux (adsorbent) et adhèrent à la structure cristalline du solide. Dans ce système la vapeur d`eau est adsorbée sur l`alumine activée. L`adsorbant a été sélectionné basé sur des études précédentes et à cause de sa capacité élevée pour l`adsorption de la vapeur d`eau, sa grande chaleur d`adsorption et sa stabilité [Dicaire et Tezel, 2011]. Cette étude a confirmé les résultats des études précédentes et a été poursuivie afin de trouver une façon d'augmenter l`efficacité de ce procédé et de confirmer sa faisabilité et son applicabilité pour un système à grande échelle.

Dans cette thèse, divers adsorbants, des zéolites et des hybrides d`alumine activée avec différentes compositions de zéolite, ont été examinés pour trouver l`adsorbant le plus

efficace pour l`entreposage d`énergie thermique ayant une densité d`énergie maximale. Des expériences ont été menées dans deux colonnes dont le volume de la plus grosse colonne était 16 plus grand pour permettre d'étudier la mise à l'échelle. La performance du système pendant la libération d'énergie durant un cycle marche-arrêt a été étudiée pour plusieurs cycles dont la durée de fonctionnement et les périodes d'arrêt ont été variées. De plus, une simulation du procédé exothermique d`adsorption a été développée en solutionnant les bilans de masse et énergie dans la colonne, l`accumulation d`eau dans les particules d`adsorbant, et le bilan d`énergie sur la paroi de la colonne. La simulation a été vérifiée en comparant les résultats expérimentaux des deux colonnes pour différents débits volumétriques. Finalement, une conception d`usine et les estimations des coûts d`immobilisation et des coûts d`énergie thermique ont été faits pour une usine d`entreposage d`énergie thermique par adsorbant. Une étude économique a été faite pour différentes capacités et périodes de remboursement.

Table of Contents

List of Figures

List of Tables

1. Introduction, Literature Review and Objectives

1.1 Introduction

Fossil fuels, such as coal, petroleum and natural gas, form the world's primary energy source by having a share of more than 85% in total energy consumption, and this share is increasing day by day. Fossil fuels are non-renewable energy sources as they take millions of year to form, and currently, reserves are being depleted much faster than the new ones are being formed. Therefore, it is expected that in the near future, world will approach a peak in fossil fuel production and consumption, causing a remarkable price increase and shortages in energy sources [Duncan, 2009].

Environmental effects of the fossil fuel combustion are also a big concern as air pollution is primarily caused by it. Principal air pollutants resulting from fossil fuel combustion are carbon monoxide, sulfur oxides, nitrogen oxides and particulate matter as they effect lungs and respiratory track, and are poisonous. Moreover, burning fossil fuels produces around 5.5 gigatonnes of carbon dioxide (CO_2) per year, and forms the 50% of the gases that are thought to be responsible for the greenhouse effect [Fossil Fuels, 2013; Kasting, 1998].

In order to alleviate the depletion risk of fossil fuels and reduce its environmental effects, share of the renewable energy sources in total energy consumption needs to be increased by improving existing systems or finding new processes. Thermal energy storage is one of these emerging processes which stores available excess thermal energy in energy storage reservoirs for later use. Thermal energy is a primary requirement for all commercial, residential, and industrial applications, especially in winter. Therefore, storing thermal energy has many benefits as it reduces the fossil fuel dependency, decreases the

greenhouse effect by reducing carbon dioxide emissions, and reduces the emissions of many air pollutants such as carbon monoxide, sulfur oxides, nitrogen oxides, and particulate matter [Dincer and Rosen, 2002].

The focus of this thesis has been investigating thermal energy storage system in adsorbent beds, checking its feasibility in larger scales, modeling the process and confirming that this model can be applied for processes at different flow rates and with different scales, and finally, doing an overall plant design and carrying out the economic analysis for the system to obtain a realistic thermal energy price.

1.2 Literature Review

1.2.1 Adsorption

Adsorption is a physical process that involves binding of molecules or particles onto a solid surface. During adsorption, one or more molecules of a gas or liquid stream are adsorbed on the surface of a solid adsorbent and a separation is accomplished. Overall adsorption process occurs in three steps. Firstly, adsorbate diffuses from the bulk fluid to the exterior surface of the particle (adsorbent). Then, adsorbate diffuses inside the pores, and finally, adsorbate is adsorbed in the pores. When all the pores of an adsorbent are filled with adsorbate (when it is saturated), regeneration is done by passing a hot fluid through the bed or by reducing the pressure in the adsorption column to remove the adsorbates and make the adsorbent ready for the next process [Geankoplis, 2003]. A schematic explanation of this process is given in Figure 1.1.

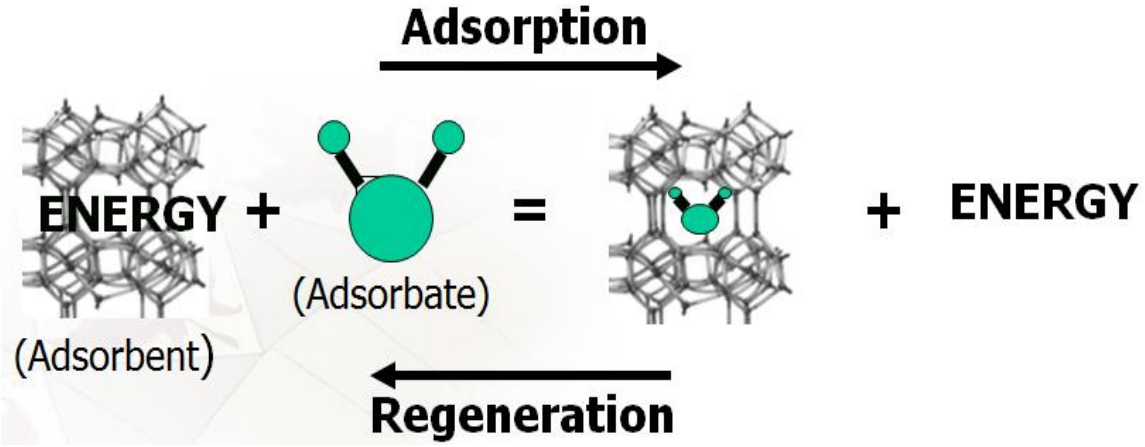

Figure 1.1: Schematic explanation of adsorption and regeneration processes [Dicaire,2010].

Adsorbent is usually in the form of small particles that has porous nature which provides a high surface area, and thus, high adsorption capacity [Geankoplis, 2003]. There are various kinds of adsorbents, such as activated carbons, zeolites, activated alumina, and silica gels, which are used in several industrial purification or separation processes. The adsorbate/adsorbent pair is chosen carefully considering adsorbent's heat of adsorption, adsorption capacity and affinity for each adsorbate [Cavalcante, 2000].

1.2.2 Thermal Energy Storage Systems

Thermal energy storage allows storing energy to be used for heating or cooling for later use. This storage process occurs in three steps: (1) charging the storage medium with excess energy, (2) storing the charged energy, and (3) discharging when the stored energy is required. A regular thermal energy storage system consists of three parts: (1) a storage material, (2) a heat exchanger for charging and discharging the material, and (3) a container enclosing the storage medium. Efficiency, thus cost of a thermal energy storage

system depends on multiple factors such as energy density (storage capacity) and stability of the storage material, heat transfer between the charging or discharging fluid and the storage material, reversibility of the system, and the amount heat loss [Cabeza, 2012]. Thermal energy storage can be done in three different processes: sensible heat storage, latent heat storage, and thermo-chemical heat storage.

In sensible heat storage systems, storage material is heated or cooled down, and as the amount of stored heat changes, temperature of the material varies. Therefore, efficiency and the cost of this method depend on mass, heat capacity, stability and cost of the storage material, the temperature difference between the material and the ambient, and the amount of insulation used to reduce the heat loss during the storage period. Storage materials that are used in sensible heat storage systems are divided into two categories: (1) liquid media such as water, oil based fluids and molten salts, and (2) solid media such as rocks and metals. In industrial applications of this process, either excess solar energy received during a bright summer day is stored to be used at nights and in winter or waste heat obtained from power plants is stored [Hasnain, 1998]. These storage processes are done with various methods such as borehole storage in which solar energy is stored, aquifer thermal energy storage in which cold storage is done, and cavern and pit storages which are currently being developed [International Energy Agency, 2006].

Sensible heat storage systems are extremely cheap processes, and currently the most dominant thermal energy storage methods. However, they have really low energy densities between 10-50 kWh/m^3 which cause the requirement of very large volumes for

commercial storage systems. A comparison of sensible and latent heat storage systems' required storage medium volumes in order to store 300 kWh is given in Table 1.1 [Hasnain, 1998]. Also, as the discharge temperature of sensible heat storage system varies with respect to time, and as there is a constant heat loss to the surrounding, it is not an applicable process for long-term energy storage [Dicaire, 2010].

Table 1.1: Comparison of sensible and latent heat storage systems for storing 300 kWh [Hasnain, 1998].

	Sensible Heat Storage		**Latent Heat Storage**	
Property	**Rock**	**Water**	**Organic**	**Inorganic**
Latent heat of fusion (kJ/kg)	*	*	190	230
Specific heat (kJ/kg)	1.0	4.2	2.0	2.0
Density (kg/m^3)	2240	1000	800	1600
Storage mass for storing 300 kWh, (kg)	67000	16000	5300	4350
Relative mass**	15	4	1.25	1.0
Storage volume for storing 300 kWh,m^3	30	16	6.6	2.7
Relative volume**	11	6	2.5	1.0

* Latent heat of fusion is not of interest for sensible heat storage.

** Relative mass and volume are given based on latent heat storage in inorganic phase change materials, whose relative mass and volume are 1.0.

Latent heat storage is a particularly more attractive technique than sensible heat storage as it has higher energy densities thus requires smaller volumes, and can discharge heat at a

nearly constant temperature. In latent heat storage systems, energy is stored while phase change materials undergo solid – solid, liquid – gas, and solid – liquid phase transformations. Generally, solid – liquid transformation (melting/solidification) is used as it can store much more heat over a narrow temperature range, and does not require large volumes like sensible heat storage systems or liquid – gas transformations. Latent heat storage system is composed of three components: (1) a heat storage material that undergoes phase transitions, (2) a heat exchanging surface that transfers heat from the source to the phase change material, and (3) a container that encloses the material [Hasnain, 1998]. In industrial applications of latent heat storage systems, paraffin waxes, which have energy densities around 100 kWh/m^3, are generally used. In those processes, paraffin waxes, which are attached to building walls, store cooling energy by getting cooled and solidified during the summer nights, and during the day, they use this stored energy to cool the building walls, and thus the whole building, reducing the need for air conditioning [International Energy Agency, 2006]. Moreover, some high melting point phase change materials, such as molten salts and metals, are used in high temperature applications and have energy densities as high as 500 kWh/m^3. However, those materials are suitable for steam production instead of residential applications [Hoshi et al., 2005].

Thermo-chemical energy storage systems use endothermic/exothermic processes such as chemical reactions and sorption processes to store energy. While storing heat by chemical reactions, firstly, dissociation reaction is done to store excess energy, and then recovery (release) of this stored energy is done by reverse reaction. Sorption systems are also considered as thermo-chemical heat storage systems as they are based on chemical

processes. In adsorption thermal energy storage systems, regeneration energy, which is used to reactivate the saturated adsorbents for the adsorption process, is stored. When the thermal energy is needed, exothermic adsorption process is carried out in order to release the stored energy and heat the space or water. Thermo-chemical energy storage systems have higher storage densities than the other types of thermal energy storage systems which allow large quantities of energy storage in small volumes for residential applications. Those systems are specifically appropriate for long – term storage applications as the energy is stored as chemical potential, it does not degrade with time, eliminating the heat loss during the storage period [Abedin and Rosen, 2011].

1.2.3 Applications of Thermal Energy Storage Systems in Adsorbent Beds

Thermal energy storage in adsorbent beds has a wide application range as excess energy supplied from any source can be stored by using this technology. The most feasible two options are: seasonal storage of solar energy for residential and commercial applications, and excess thermal energy storage in power plants and transporting it to another location. In both applications, water vapor adsorption from ambient air is selected as the energy storage process due to being economical and having safe raw materials. In previous studies, hybrid adsorbent of activated alumina and zeolite was selected for this process due to its high heat of adsorption, high water adsorption capacity, stability, and price [Dicaire and Tezel, 2011].

In seasonal solar energy storage scenario, excess solar thermal energy that is collected during summer months is stored in adsorbent beds. This storage (charging the system) is

done by heating air up to the regeneration temperature (with this energy to be stored) and passing it through the column to desorb all the water from the adsorbent bed. When the stored thermal energy is needed to be discharged in winter or at nights, exothermic adsorption process (adsorption of water by the adsorbent bed) is carried out. This process heats up the dry air that carries the water vapor through the column. Then, this heated dry air can be used in space heating or hot water tank heating. In Figure 1.2, amount of solar energy that can be collected from PS35 solar collector (from Menova Energy Inc.) in a typical single family Canadian home in Montreal during the year is compared with the thermal energy requirements of this home with and without including the domestic hot water (DHW) heating requirements. As seen from this graph, there is a remarkable amount of excess energy available in summer months, and this energy can be stored and used in winter to eliminate the thermal energy dependency of the house to fossil fuels.

All power plants use combined heat and power units to produce electricity and thermal energy. In those units, firstly, fuel combustion is done. Exhaust gas from the combustor, which is around 1000^{o}C, enters the turbine for electricity production. After electricity is produced, exit temperature of the turbine goes down to around 400^{o}C, and then this exhaust gas passes through the heat exchanger for thermal energy production [Boyce, 1982]. However, 30% of the thermal energy discharged from the heat exchanger is excess and directly released to the atmosphere as heat loss [Waste Heat to Power Systems, 2013]. A schematic diagram of this electricity and thermal energy production process is given in Figure 1.3.

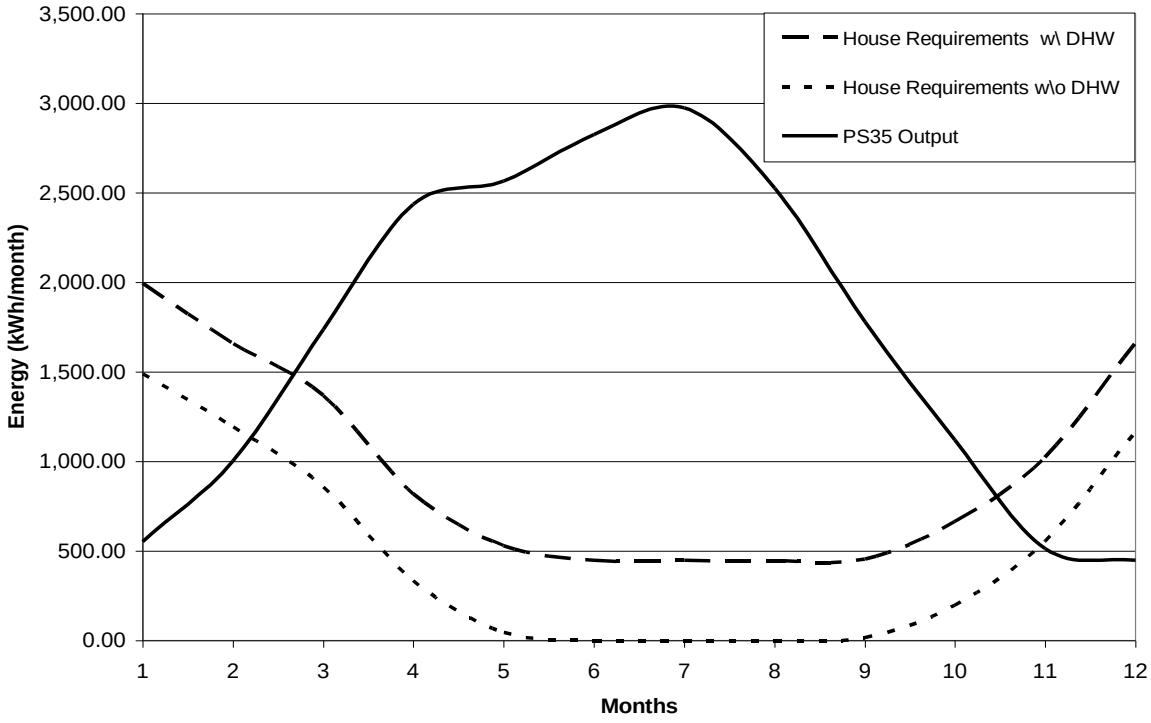

Figure 1.2: Monthly thermal energy requirements of a single family home in Montreal, Canada with and without domestic hot water (DHW) compared to the monthly thermal energy output of a PS35 solar collector (from Menova Energy Inc.) attached to the same home [Dicaire, 2010].

Excess, low quality thermal energy produced by the power plants can be stored in adsorbent beds, and those adsorbent beds which are ready to release thermal energy can be transported to residential and commercial buildings nearby. Moreover, this portable system eliminates the two problems that adsorption thermal energy storage system has: (1) space needed to install the system, and (2) the capital cost of the whole installation.

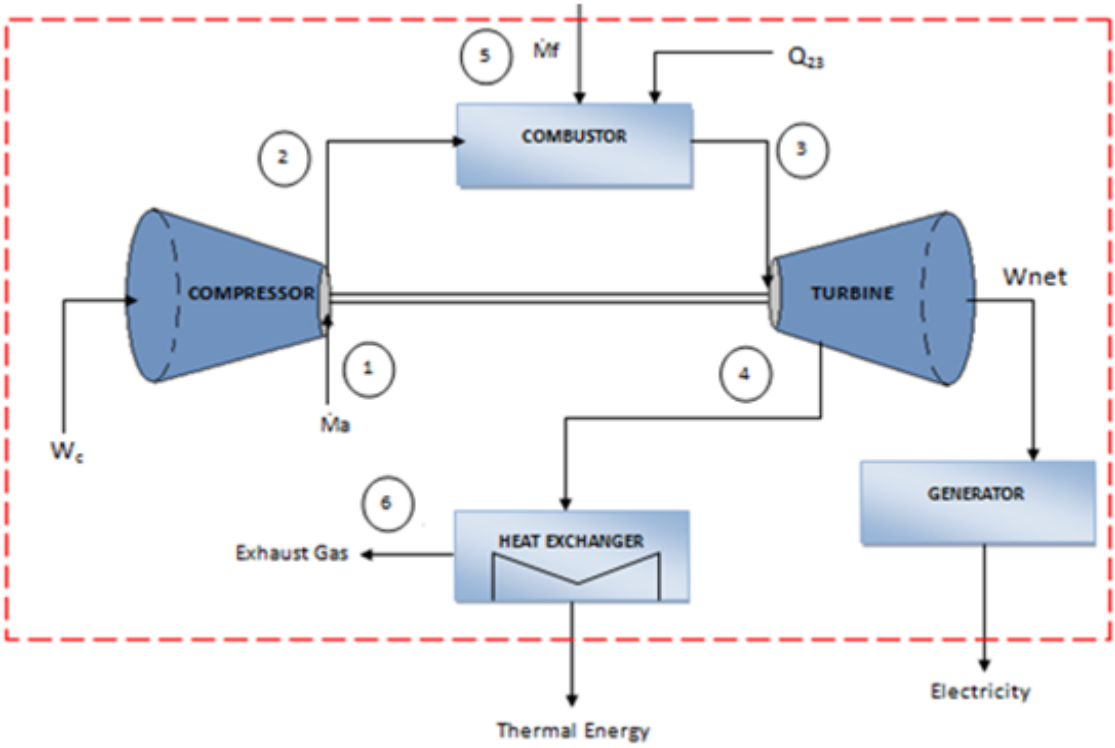

Figure 1.3: Schematic diagram of a combined heat and power (CHP) unit [Boyce, 1982; Sandler, 2006].

An open adsorption system for thermal energy storage has been installed in Munich, Germany in order to heat a school building which has a size of 1625 m^2. An adsorption column in a size of 7 m^3 is used in this system, and due to its high water adsorption capacity, zeolite 13X is used as adsorbent for the column. In this process, energy storage (regeneration) is done at nights, when there is less demand for thermal energy, by using the steam line of the district heating system. This regeneration process is done around 130^oC, and waste heat of the regeneration process (exiting hot air from the column) is supplied to the heating system of the school. In day time, when there is a peak thermal energy demand, the stored energy is discharged by passing humidified (saturated) air through the adsorption column. In this process, air enters the column at around 25^oC –

30^{o}C and exits around 65^{o}C which was directly transferred to the heating system of the school. Energy density of this storage system was reported to be 124 kWh/m^{3} [Hauer, 2002]. This obtained energy density was increased in previous studies by using zeolite and activated alumina hybrid material as adsorbent, as activated alumina increased the heat of water adsorption of the system while zeolite provided high water adsorption capacities [Dicaire and Tezel, 2011].

Another open adsorption system has been integrated into a dishwasher with the collaboration of ZAE Bayern and Bosch Siemens Hausgerate in Germany. In a regular dishwasher, there exist two heating processes: (1) for washing process (around 50^{o}C) and (2) for drying process (around 60^{o}C). The purpose of using adsorption in dishwashers is to eliminate the second heating process and dry the dishes by using the hot and dry air obtained from water vapor adsorption. This drying is done by blowing the humid air available in the dishwasher after the washing process into the adsorption column to produce hot and dry air. This air is then used for dishwasher drying and when the column is completely saturated, drying process finishes. After the column is saturated, regeneration is done by using the thermal energy available during the first heating process. As a result, this integrated dishwasher system reduces the energy demand of a regular dishwasher by 23% [Hauer and Fischer, 2011].

1.3 Objectives

In previous studies carried out in our lab on thermal energy storage system in adsorbent beds, optimum conditions for this process, and feasibility of the technology was validated [Dicaire and Tezel, 2011]. The objectives of this thesis have been:

- To find a more efficient adsorbent for this system in order to achieve an energy density higher than 200 kWh/m^3.

- To confirm the applicability of this system in larger scales by replacing the existing column with a bigger one and proving that same energy densities can be achieved with different column volumes.

- To investigate the feasibility of on-off heat release in adsorption thermal energy storage systems by performing on-off experiments at different on-off time periods.

- To model the exothermic adsorption process by performing mass and energy balances for the system.

- To confirm the validity of the model by comparing experimental and modeling results at different flow rates and at different column volumes.

- To make an overall plant design and economic analysis of the plant to obtain a realistic installation cost for the system at different energy storage capacities.

- To calculate a price for the stored thermal energy for different thermal energy storage capacities and payback periods to decide on the feasibility of the system by comparing this price with current electricity prices.

1.4 References

Abedin, A. H., Rosen, M. A. (2011). “A Critical Review of Thermochemical Energy Storage Systems”. The Open Renewable Energy Journal, 4, 42-46.

Akgun, M., Aydin, O., Kaygusuz, K. (2007). “Experimental study on melting/solidification characteristics of a paraffin as PCM”. Energy Conversion and Management, 48, 669-678.

Boyce, M. P. (1982). “Gas Turbine Engineering Handbook”. Gulf Publishing Company, Houston, Texas.

Cabeza, L. F. (2012). “Thermal Energy Storage”. Comprehensive Renewable Energy, 3, 211-253.

Cavalcante, C. L. JR. (2000) “Industrial Adsorption Separation Processes: Fundamentals, Modeling and Applications”. Latin American Applied Research, 30, 357-364.

Dicaire, D. N. (2010) “Long Term Thermal Energy Storage in Adsorbent Beds for Solar Heating Applications”. M.A.Sc. Thesis, University of Ottawa, Ottawa, Canada.

Dicaire, D. N., Tezel, H. F. (2011) “Regeneration and efficiency characterization of hybrid adsorbent for thermal energy storage of excess and solar heat”. Renewable Energy, 36, 3, 986-992.

Dincer, I., Rosen, M. A. (2002). “The role of Thermal Energy Storage Systems and Applications”. John Wiley & Sons, New Jersey.

Duncan, R. (2009). “The City of Austin Energy Depletion Risks Task Force Report”. Austin Energy, Texas, U.S.

Fossil Fuels: Environmental Effect. Retrieved on March 28, 2013 from http://www.ems.psu.edu/~radovic/Chapter11.pdf

Geankoplis, C. J. (2003). “Transport Processes and Separation Process Principles”. Prentice Hall, New Jersey, U.S.

Hasnain, S. M. (1998). “Review on sustainable thermal energy storage technologies, Part l: heat storage material and techniques”. Energy Conversion and Management, 3, 11, 1127-1138.

Hauer, A. (2002). “Thermal energy storage with zeolite for heating and cooling applications.” Proceedings of the 7th International Sorption Heat Pump Conference ISHPC, 385-390, Shanghai.

Hauer, A., Fischer, F. (2011). “Open Adsorption System for an Energy Efficient Dishwasher.” Chemie Ingenieur Technik, 83, 61-66.

Hoshi, A., Mills, D. R., Bittar, A., Saitoh, T. S. (2005). ‘Screening of high melting point phase change materials (PCM) in solar thermal concentrating technology based on CLFR”. Solar Energy, 79, 332-339.

International Energy Agency, Energy Conservation through Energy Storage Programme, March 2006. Downloaded on March 27, 2013 from http://www.iea-eces.org/files/brochure06.pdf

Kasting, J. F. (1998) “The Carbon Cycle, Climate, and the Long-term Effects of Fossil Fuel Burning”. Consequences, 4, No:1.

Sandler, S. I. (2006). Chemical, Biochemical, and Engineering Thermodynamic. John Wiley & Sons, New Jersey.

Waste Heat to Power Systems, Retrieved on March 2, 2013 from http://www.epa.gov/chp/documents/waste_heat_power.pdf

Zalba, B., Marin, J. M., Cabeza, L. F., Harald, M. (2003). “Review on thermal energy storage with phase change: materials, heat transfer analysis and applications”. Applied Thermal Engineering, 23, 3, 251-283.

2. Thermal Energy Storage in Adsorbent Beds:

Investigation for Different Adsorbents, Different Columns, and

On-Off Experiments

ABSTRACT

Thermal energy storage system in adsorbent beds is a promising technology as it enables the storage of solar energy received during the summer (or during the day) or the storage of excess, low quality thermal energy obtained from power plants. This system stands out from other thermal energy storage systems as heat storage in adsorbent beds eliminates the heat loss with respect to storage time, and more than 50 cycles can be performed in one bed without any performance loss [Dicaire and Tezel, 2011].

In this chapter, literature data available for this system is confirmed. Energy density of 204.5 kWh/m^3 is obtained for the hybrid adsorbent of activated alumina and zeolite at an optimum flow rate of 24 L/min, inlet air relative humidity of 100%, and after performing regeneration run at 250^oC. Then, 7 different compositions of hybrid activated alumina and zeolite adsorbent are investigated, and concluded that alkaline addition and increasing activated alumina percentage increases energy density up to 226.1 kWh/m^3. Moreover, in order to confirm the feasibility of this system in larger scale applications, existing 62.76 mL column is replaced with a 1 L column. Optimum energy density of 203.7 kWh/m^3 at a flow rate of 30 L/min is obtained confirming the applicability of this system in larger scales.

Releasing all of the stored thermal energy at once may not be useful for real time applications. Therefore, on-off experiments for different time periods are performed. It is concluded that this decreases the energy density to 187.8 kWh/m^3. However, this decreased value is still efficient as it has a higher energy density than many other thermal energy storage methods, and it enables us to control the release of the stored heat.

2.1 Introduction

Currently, more than 85% of thermal energy demand of the world is supplied from fossil fuels. However, fossil fuels are non-renewable, and our rate of consumption is much higher than their formation rate which confronts us with the depletion risk of those fuels [Duncan, 2009]. Moreover, fossil fuel combustion has serious health effects as it causes the release of hazardous gases such as carbon monoxide, sulfur oxides, nitrogen oxides and particulate matter. Fossil fuels are also responsible for forming the more than 50% of the world's carbon dioxide emissions that are causing the greenhouse effect [Kasting, 1998]. Thus, depletion risk, health and environmental effects of fossil fuels force humankind to find other energy sources such as renewables.

Renewable energy comes from the sources that are continuously replenished such as sunlight, wind, waves, rain, biomass and waste energy. In literature, it is estimated that by 2050, renewable energy production will increase and be able to supply 40% of the world's energy consumption. Total renewable energy production will be shared in several sources as follows: 64% will be supplied from biomass, 24% will be supplied from hydroelectricity, and the remaining 12% will be supplied from other sources such as solar and geothermal [Johansson et al., 1993]. Those low percentages show that renewable sources are not efficient enough to replace natural sources. Therefore, in order to make a remarkable reduction in fossil fuel dependency, new technologies are needed in addition to the existing renewable processes.

Thermal energy storage is one of those developing technologies and it is carried out with three different methods: sensible heat storage, latent heat storage, and thermo-chemical heat storage. In sensible heat storage systems, a material, like rock, is heated in an insulated container. This storage method is currently the most used process due to its economic feasibility. However, as there is a continuous heat loss to the environment during the storage period, it cannot be applied for long-term energy storage [International Energy Agency, 2013]. Another method used is latent heat storage. In latent heat storage systems, energy released during the phase change of a material is used. This method has many advantages such as having energy densities up to 500 kWh/m^3, and discharging stored thermal energy at nearly constant temperatures. However, this process is designed for high temperature processes such as steam production and cannot be applied for residential processes [Hoshi et al., 2005]. Finally, thermo-chemical heat storage systems use exothermic/endothermic processes to store heat. As thermal energy is stored as chemical potential during the endothermic process, energy does not degrade with time. When the thermal energy is required, exothermic process is performed. [Abedin and Rosen, 2011].

Thermal energy storage in adsorbent beds is a thermo-chemical heat storage method in which exothermic water vapor adsorption from air is performed to heat flowing air which then can be used for space or water tank heating. In adsorption, adsorbate (water vapor) diffuses into the pores of a porous solid material (adsorbent) and gets trapped in the crystal lattice which is referred as the adsorbed phase. Fluid is passed through the adsorbent bed until all the pores are filled with the adsorbate. Then, regeneration is done by passing hot fluid through the adsorbent bed in order to remove the trapped adsorbates

from the pores and get the adsorbent bed ready for the next heat releasing adsorption process [Geankoplis, 2003].

Aside from the thermal energy storage systems, there are several applications that adsorption processes are used such as carbon dioxide and sulfur removal, water pollution control, and various gas and liquid separation processes. Adsorbents that are used in those processes are selected due to their affinities for a specific adsorbate, adsorption capacities, and heats of adsorption. For thermal energy storage systems, hybrid adsorbent of activated alumina and zeolite is found to be the most efficient adsorbent due to its high heat of adsorption supplied from activated alumina, and high adsorption capacity coming from zeolite [Kim and Lee, 2003].

In this chapter, after confirming the energy density values found in previous studies, various compositions of hybrid adsorbent are investigated in order to find a more efficient adsorbent that gives a higher energy density. Then, applicability of this system into larger scales is studied by performing adsorption experiments both in small and 16 times larger columns. Also, applicability of on-off heat release in adsorption is looked at, as well.

2.2 Experimental Setup

Experimental procedure is composed of mainly two steps: adsorption and regeneration. During adsorption, air supply, which comes from the air compressor of the building, passes through the air filter in which solid particulates are separated. This filtered air then enters the bubbler to increase its relative humidity to around 97% by using an ultrasonic fog generator. In this step, temperature of the air increases around $5^{o}C$ because of the

warming up of the fog generators while working. In order to prevent water droplets from entering the adsorption column, humid air exiting the bubbler enters into a water trap. To obtain a constant relative humidity before starting the adsorption process, bypass line (valves 6) is used. After measuring a stable relative humidity value, bypass is closed, and valves 4 and 5 are opened to start the adsorption. Then, humid air enters column and exits as heated, and dry. (Outlet humidity increases gradually with respect to time, and air is heated up to around 80^{o}C.)

During the regeneration process, air again passes through the air filter to remove the solid particulates. Then, it enters to an in-line air heater and heated to the most efficient regeneration temperature of 250^{o}C [Dicaire and Tezel, 2011]. This heated air is passed through the saturated adsorption column in order to evaporate the condensed water in the pores and regenerate the column. Hot air is continuously passed through the column until the outlet air humidity reduces to 0% relative humidity.

Schematic diagram of this process is given in Figure 2.1. Inlet and outlet temperatures of the air, as well as the temperature at different positions in the column are measured by thermocouples throughout the experiment to obtain a temperature profile with respect to time. Readings obtained from thermocouples are used to calculate the total amount of energy released from the column during adsorption. Energy released at each data point at different times is calculated by using the difference between column inlet and outlet temperatures, flow rate, heat capacity and density of the process air at that point. Then, total energy released during adsorption is simply calculated by adding these energy

released values calculated at different times during the adsorption run. Finally, energy density is calculated by dividing the total amount of energy released by the column volume for the particular pellet size used.

In order to obtain outlet humidity versus time graphs both for adsorption and regeneration processes and the adsorption capacity of the adsorbents, humidity of the exiting air from the column is measured continuously. Adsorption capacities of the adsorbents are calculated by using the differences between the humidities of column inlet (at 100% relative humidity) and outlet air at different times as well as the air flow rate and the amount of adsorbent in the column. To ensure a correct humidity value, before reading its relative humidity, air is passed through a cooling coil to obtain a constant air temperature. As this process causes condensation through the end of the adsorption process, exiting air with water droplets enters the hygrometer container which has a volume enough to hold condensed liquid to make sure all the humidity going out is measured.

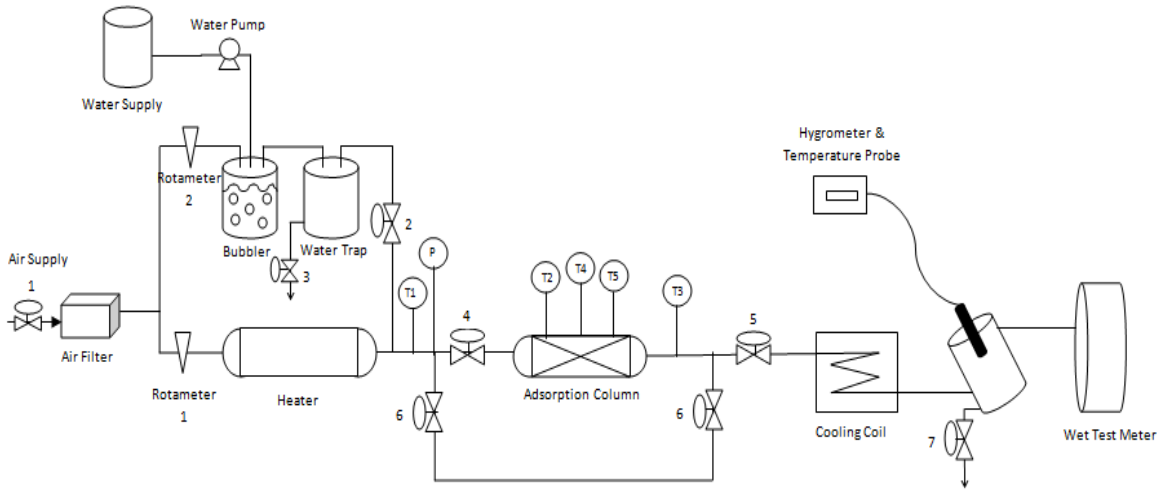

Figure 2.1: Schematic diagram of the experimental setup

While conducting the experiments, the same experimental setup was used as Dicaire and Tezel with few modifications [Dicaire and Tezel, 2011]. Few experiments were carried out with the existing 62.76 mL column (with L/D ratio of 1.8) in order to validate the experimental results of previous studies and search for a better adsorbent. Then, this column was replaced with a 16 times bigger one (volume of 1 L, and L/D ratio of 2.8). Two new thermocouples were added to the big column's surface to get a detailed temperature profile during adsorption. As the water level of the bubbler decreases because of the mist generation from the foggers, a water supply line to the bubbler, a water pump, and a water container was added to the system. Hybrid adsorbent of zeolite and activated alumina was used for adsorption. Finally, a fine mesh was attached in the middle of the hygrometer container in order to prevent condensed water from splashing to the high temperature and relative humidity probe.

Inlet air comes from the air compressor of the building supply which produces quality air with little humidity (3 to 4% relative humidity). Rotameters 1 and 2 control the dry and humid air supplies to the system, respectively. All of the tubing in the system is 1/4" tubing. Silicone and polyethylene tubing are used in the parts at around ambient temperature and stainless steel is used for the parts at high temperatures. The existing column from the setup of Dicaire and Tezel has a 38.1 mm outer diameter and 70 mm length [Dicaire and Tezel, 2011]. The new column has a length of 24.1 cm and an outer diameter of 8.8 cm. Both columns are made out of Stainless Steel 314 and have 1/4" pipes welded at the entrance and the exit. The bubbler is a 4 L cylindrical container which contains a Hagen Exo Terra Ultrasonic Fog Generator. Fogger sits in around 8 centimeters of water and increases

the flowing air's relative humidity up to 97%. The heater is an in-line air heater AHP-5051 from Omega which is connected to a rheostat which enables the stabilization of the temperature of the flowing air. Humidity was measured with a high temperature and relative humidity probe transmitter (HX-15W) supplied from Omega. Rotameters' calibration was done by using Precision Wet Test Meter.

2.3 Results and Discussion

In previous studies on this project, optimum conditions for the small 62.76 mL column were found. In order to obtain the highest energy density of 200 kWh/m^3, column has to be filled with hybrid adsorbent of activated alumina and zeolite (Activated alumina is used due to its high heat of adsorption for water vapor, and zeolite is used due to its high water adsorption capacity.), regeneration has to be done at 250^oC, volumetric flow rate of the inlet air stream has to be 24 L/min, and inlet air stream has to have 100% relative humidity [Dicaire and Tezel, 2011]. Before doing any further studies, these results are confirmed. As seen from the energy density versus volumetric flow rate graph shown in Figure 2.2, optimum flow rate for the 62.76 mL column is again found to be 24 L/min, and energy density at that flow rate is calculated as 204.5 kWh/m^3, which confirms the previous data.

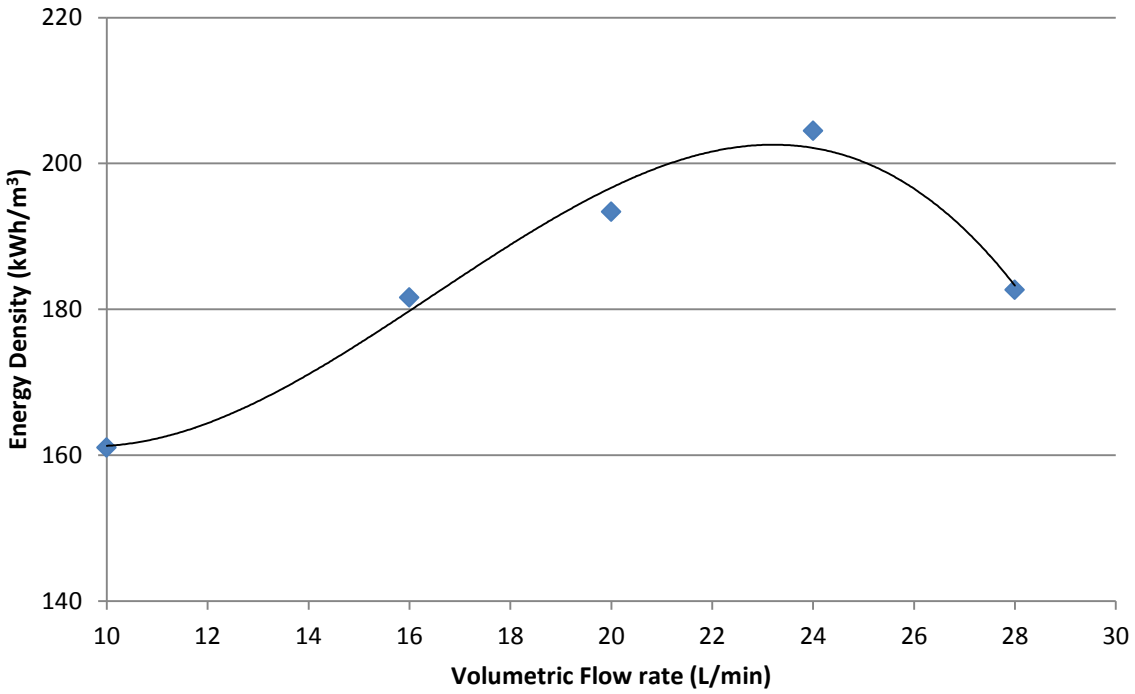

Figure 2.2: Energy density versus volumetric flow rate graph that confirms the optimum conditions and highest energy density value found in previous studies for the 62.76 mL column

Efficiency and thus the energy density of a thermal energy storage process by water vapor adsorption highly depend on the type of the adsorbent used in the column. It is found that pure zeolites have remarkably higher water adsorption capacities (around 0.29 g/g) than aluminas (around 0.14 g/g) [Breck, 1974]. Furthermore, aluminas' heats of water adsorption vary between 69.9 kJ/mol and 190.2 kJ/mol while zeolites have significantly lower heats of water adsorption between 70.8 kJ/mol and 95.1 kJ/mol [Breck, 1974; Hendriksen et al., 1972]. Therefore, it is concluded that zeolites are elevating the energy density of the system due to their high water adsorption capacities while aluminas are contributing with their high heats of water adsorption.

Different compositions of the hybrid adsorbent are investigated in order to find a better adsorbent that gives a higher energy density. Adsorption experiments are performed at the confirmed optimum flow rate of 24 L/min, with an inlet air humidity of 100% relative humidity, and are carried out for 7 different adsorbents: 1) hybrid adsorbent of activated alumina and zeolite, 2) hybrid adsorbent of activated alumina and zeolite with alkaline treatment, 3) hybrid adsorbent of more activated alumina and less zeolite with alkaline treatment, 4) alkaline added differently to the hybrid adsorbent of more activated alumina and less zeolite, 5) pure activated alumina 6) activated alumina with alkaline, and 7) activated alumina with a higher amount of alkaline within the adsorbent (6). A summary for the used adsorbents are given in Table 2.1.

Table 2.1: Compositions of the 7 different adsorbents studied

Adsorbent Type	Adsorbent Composition	Alkaline Addition
1	Activated Alumina + Zeolite	None
2	Activated Alumina + Zeolite	Type I
3	More Activated Alumina + Less Zeolite	Type I
4	More Activated Alumina + Less Zeolite	Type II
5	Activated Alumina	None
6	Activated Alumina	Type II
7	Activated Alumina	Type II (added in higher amounts)

Bar graphs given in Figures 2.3 and 2.4 show the difference between energy densities and water adsorption capacities of the 7 different adsorbents studied in this thesis. A higher energy density is obtained for the second adsorbent (204.5 kWh/m^3) compared to the first one (173.4 kWh/m^3) as alkaline addition increases the water affinity, and thus the water adsorption capacity of the adsorbent from 0.20 g/g to 0.27 g/g. Then, adsorbents 2 and 3 which have the same amount and type of alkaline but different activated alumina and zeolite percentages are compared. Even the adsorption capacity of the adsorbent bed decreases from 0.27 g/g to 0.19 g/g due to the decrease in zeolite amount, a higher energy density is obtained as the heat of adsorption increases due to the increase in activated alumina percentage. Furthermore, for adsorbents 3 and 4 in which alkaline addition is done by different methods are compared, energy densities of 217.9 kWh/m^3 and 218.5 kWh/m^3 are obtained, respectively. Also, similar adsorption capacities of 0.19 g/g and 0.18 g/g are obtained for adsorbents 3 and 4, respectively. Due to those similarities, it is concluded that the method of alkaline addition does not have a significant effect on adsorption capacity and energy density of the adsorbents.

Pure activated alumina (adsorbent type 5) is also investigated for water vapor adsorption, and energy density. By comparing adsorbents 4 and 5, it is seen that there is a significant decrease in energy density from 218.5 kWh/m^3 to 174.2 kWh/m^3. Also, adsorption capacity of the bed is decreased from 0.18 g/g to 0.13 g/g. This decrease in adsorption capacity and thus, energy density of the bed occurred as the bed does not contain any alkaline or zeolite to increase its water affinity. However, this pure activated alumina has a similar energy density as the hybrid adsorbent of activated alumina and zeolite without any alkaline

treatment (adsorbent type 1). Its adsorption capacity decreases due to the absence of zeolite, but high heat of adsorption supplied from activated alumina increases its energy density.

Moreover, two activated alumina adsorbents with different alkaline amounts (adsorbent types 6 and 7) are compared, and their energy densities are 199.7 kWh/m^3 and 226.1 kWh/m^3, respectively. As the addition of the alkaline increases the water affinity and thus the water adsorption capacity of the adsorbent from 0.16 g/g to 0.18 g/g (see Figure 2.4), a higher energy density is obtained for the adsorbent type 7 when the amount of alkaline is increased. Moreover, the highest energy density of 226.1 kWh/m^3 is obtained due to the high heat of adsorption provided from the activated alumina, and a similar adsorption capacity as the 4th adsorbent supplied from high amounts of alkaline in its structure.

It is observed that these experimental results are in a good agreement with the literature search done for the properties of zeolites and aluminas as it is proven that zeolites have higher water adsorption capacities than aluminas, and aluminas have higher heats of water adsorption than zeolites. Finally, it is concluded that in order to obtain the highest energy density of 226.1 kWh/m^3, an adsorbent with a considerably high water adsorption capacity and a high heat of adsorption for water vapor must be used.

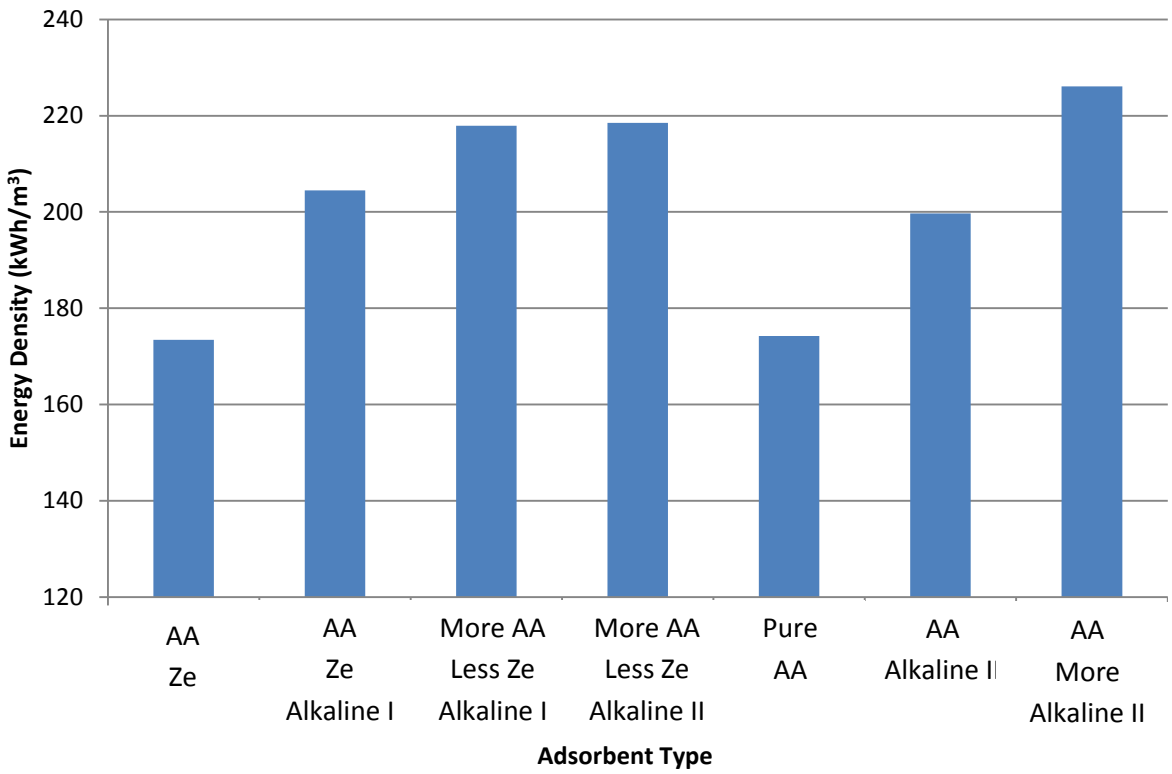

Figure 2.3: Energy density comparison of 7 different adsorbents for water vapor adsorption with inlet air of 100% relative humidity and 24 L/min flow rate

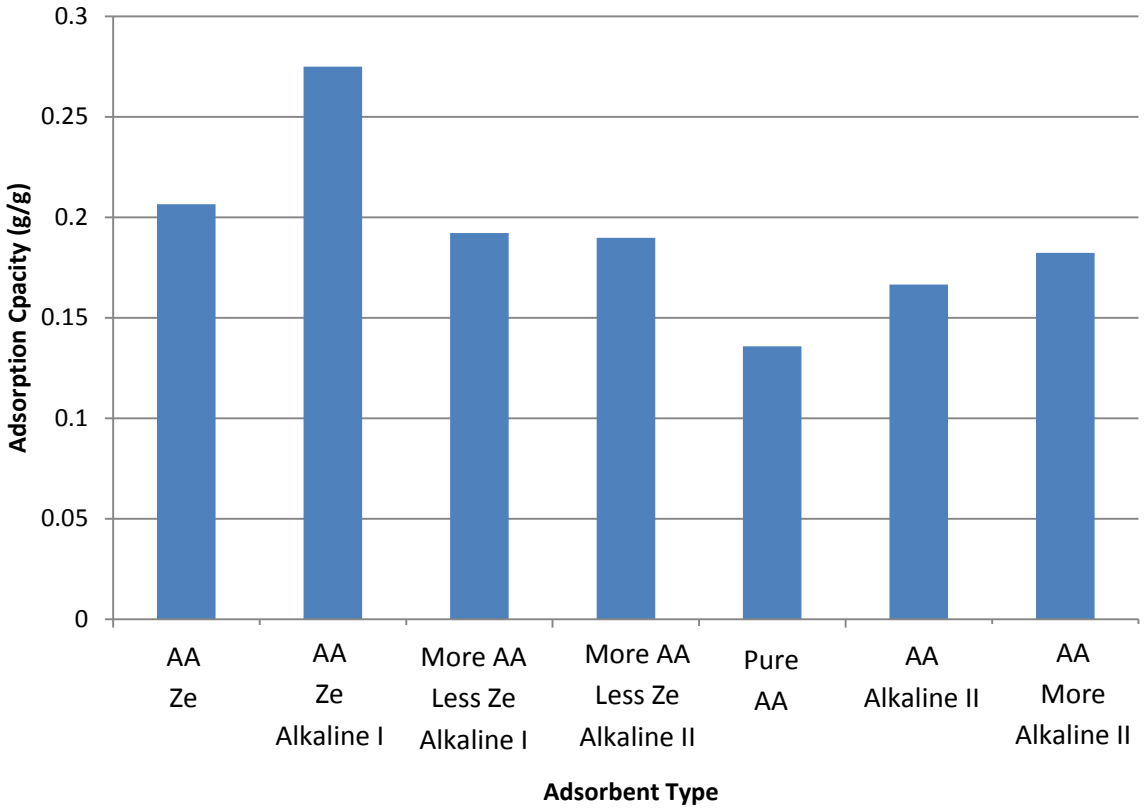

Figure 2.4: Water adsorption capacity comparison of 7 different adsorbents with inlet air of 100% relative humidity and 24 L/min flow rate

Since the main objective of this project is confirming that thermal energy storage in adsorbent beds is an applicable method, adsorption experiments are performed in larger scale. Existing column which has a volume of 62.76 mL and a L/D ratio of 1.8 is replaced with a 16 times bigger column which has a volume of 1 L, and L/D ratio of 2.8. Experiments are performed at the optimum conditions that were determined previously: regeneration at 250^{o}C, and performing adsorption with inlet air at 100% relative humidity. The column is filled with adsorbent type 4 mentioned in Table 2.1 (Hybrid adsorbent of more activated alumina and less zeolite with alkaline). As can be seen in Figure 2.5, optimum flow rate is

found to be 30 L/min, with an energy density of 203.7 kWh/m^3 as seen from this graph. A decrease in energy density from 218.5 kWh/m^3 to 203.7 kWh/m^3 is obtained due to the higher L/D ratio of the larger column. During the adsorption process, energy density is calculated by using the temperature difference of the flowing air at the column inlet and outlet. As the L/D ratio of the column increases, more energy is lost from the flowing air in order to heat the adsorbents on the way to exit, and also more energy is lost from the column walls as the column becomes more elongated. Therefore, using an adsorption column with a L/D ratio of 1 instead of 1.8 or 2.8 can give much higher energy densities. Furthermore, as the L/D ratios of the small and larger columns' are different, their cross sectional areas and thus, optimum superficial velocities are different. Therefore, a change in the optimum volumetric flow rates of the two columns is observed.

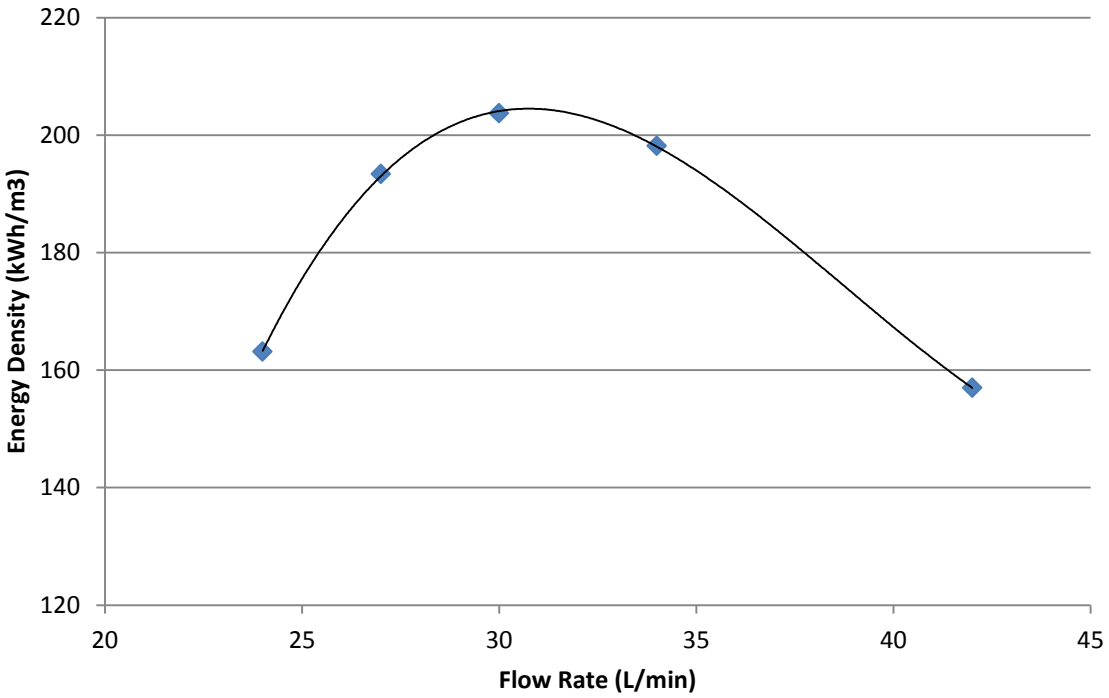

Figure 2.5: Optimum flow rate and energy density determination of 1 L column in which hybrid adsorbent of activated alumina and zeolite (adsorbent 4) is used

Figure 2.6 shows the typical breakthrough curve for the adsorption run carried out at optimum flow rate of 30 L/min. Outlet humidity is continuously measured during the experiment by using a hygrometer, and when outlet relative humidity reaches 100% (when inlet and outlet humidities become equal), experiment is stopped as the column becomes saturated and cannot adsorb more water vapor.

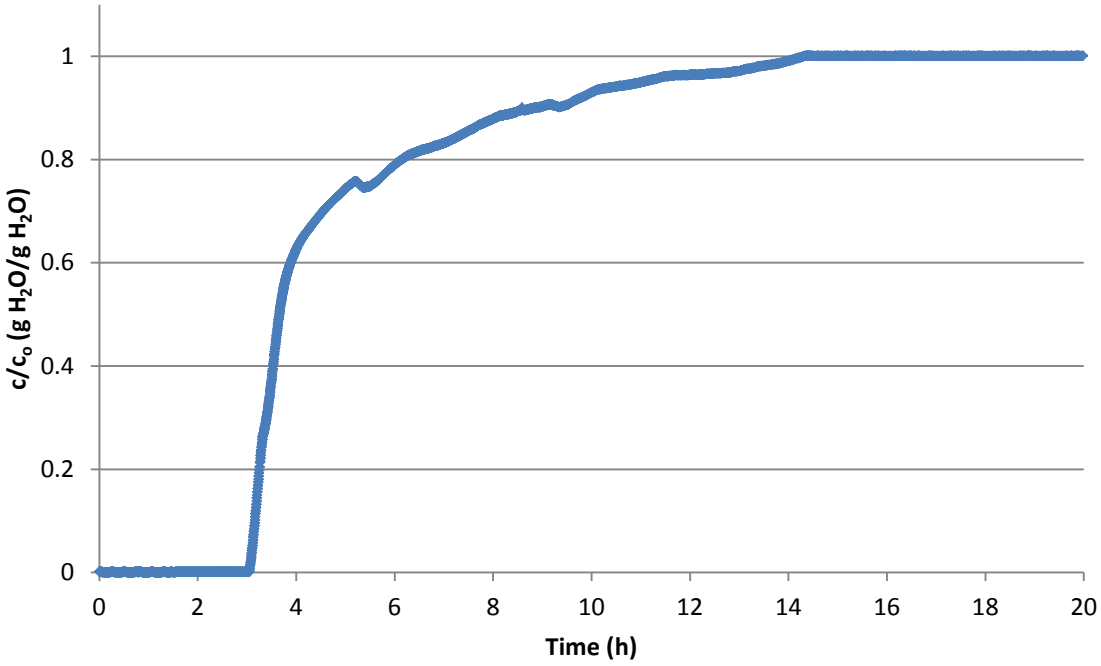

Figure 2.6: Breakthrough curve for water vapor adsorption at 30 L/min flow rate for hybrid adsorbent of activated alumina and zeolite (adsorbent 4) for 1 L column.

Figure 2.7 shows the column outlet and inlet temperatures with respect to time that is obtained during the adsorption run carried out at the optimum flow rate of 30 L/min for the larger column. Inlet humid air temperature stays fairly constant throughout the experiment, and temperature of the air passing through the column varies with respect to time due to the amount of heat released during adsorption. As the column is initially dry, it releases large amounts of energy quickly and reaches high temperatures. As the adsorbent starts to become saturated, amount of heat released due to adsorption decreases and causes a decrease in the outlet temperature. At the end of the adsorption process, inlet and outlet air temperatures become almost equal confirming that adsorbent bed is completely saturated and equilibrium has been reached.

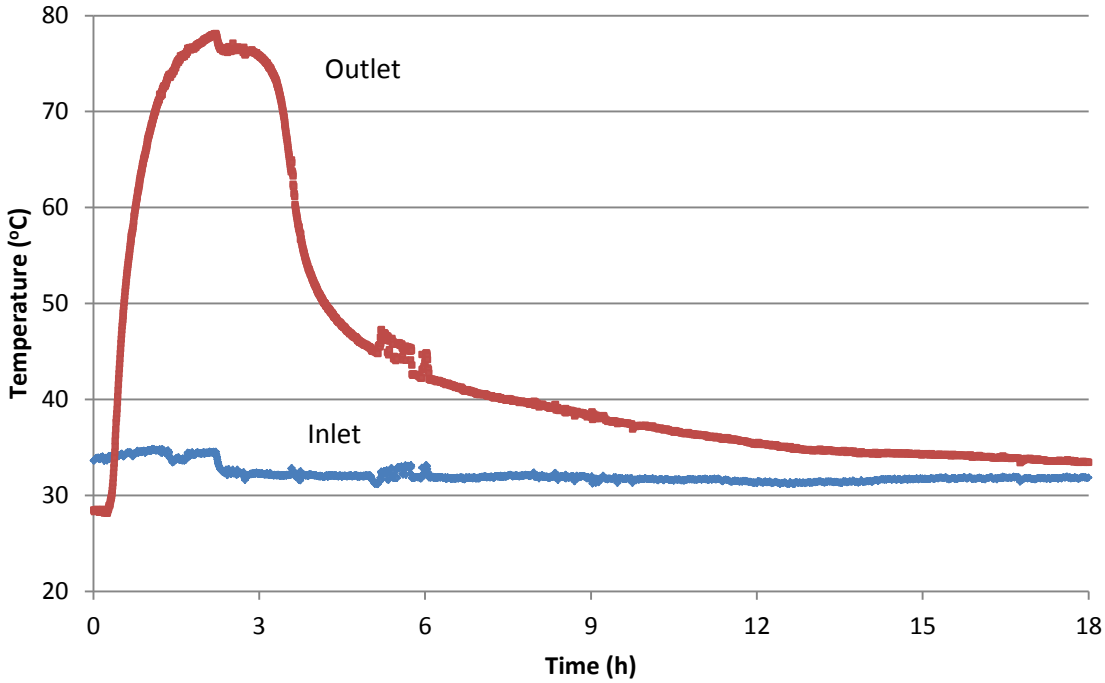

Figure 2.7: Outlet and inlet temperatures with respect to time during water vapor adsorption with hybrid adsorbent of activated alumina and zeolite (adsorbent 4) at 30 L/min flow rate for 1L column

In real time applications of this process, releasing all of the adsorption heat at once may not be practical or high amounts of thermal energy release may not be required all at once. Therefore, in order to determine the feasibility of this process in real time applications, on-off experiments are performed on 1L column. In on-off experiments, adsorption run is done at the optimum flow rate of 30 L/min, with 100% inlet air relative humidity, and with hybrid adsorbent of more activated alumina and less zeolite with alkaline (adsorbent type 4 in Table 2.1). After a previously decided period of time passes from the beginning of adsorption run, valves 4 and 5 are closed (column is isolated) and bypass line is opened. Column isolation is done for the same decided period of time. This process cycle is done

until the inlet and outlet humidities of the air become equal, and thus the column is saturated.

As seen from Figure 2.7, during an adsorption run, most of the thermal energy is released (which is indicated by the area under the temperature versus time curve in this figure) in the first 6 hours when the outlet air temperatures reaches high temperatures and a temperature bump occurs. Therefore, on-off experiments are performed by doing column isolation at different positions on the temperature bump in order to obtain more realistic results about the on-off feasibility. Thus, five different on-off time periods are chosen accordingly: 15 minutes, 30 minutes, 1 hour, 2 hours, and 3.5 hours.

Figure 2.8 shows the energy density values obtained at different on-off periods. Those on-off energy density values are compared with the energy density of a regular, non-stop adsorption run which is given in Figure 2.8 when on-off period equals to zero. We can conclude that performing on-off adsorption causes a decrease in the optimum energy density obtained compared to regular adsorption process as the highest energy density of 203.7 kWh/m^3 is decreased to 187.8 kWh/m^3. This decrease occurs due to an interruption during the temperature bump of the adsorption run. However, this decreased energy density of 187.8 kWh/m^3 is still higher than many other thermal energy storage methods. For example, in sensible heat storage systems, energy densities between 10-50 kWh/m^3 are obtained [Hasnain, 1998]. Also, in literature, several water vapor adsorption processes for thermal energy storage are performed which have energy densities lower than 187.8 kWh/m^3. An open adsorption system for thermal energy storage with an energy density of

124 kWh/m^3 was installed by Hauer in which zeolite 13X was used as the adsorbent [Hauer, 2002]. Also, Janchen and Stach obtained an energy density of 165 kWh/m^3 by performing water vapor adsorption with NaX [Janchen and Stach, 2012].

Moreover, as seen from Figure 2.8, when the on-off period increases up to 2 hours (as the on-off frequency decreases), energy density increases. However, when the column is isolated for a long time such as 3.5 hours, it causes the column to cool down to low temperatures because of heat losses, and when the adsorption is restarted, it cannot reach the high peak temperatures. This causes a remarkable decrease in the energy density obtained from the system.

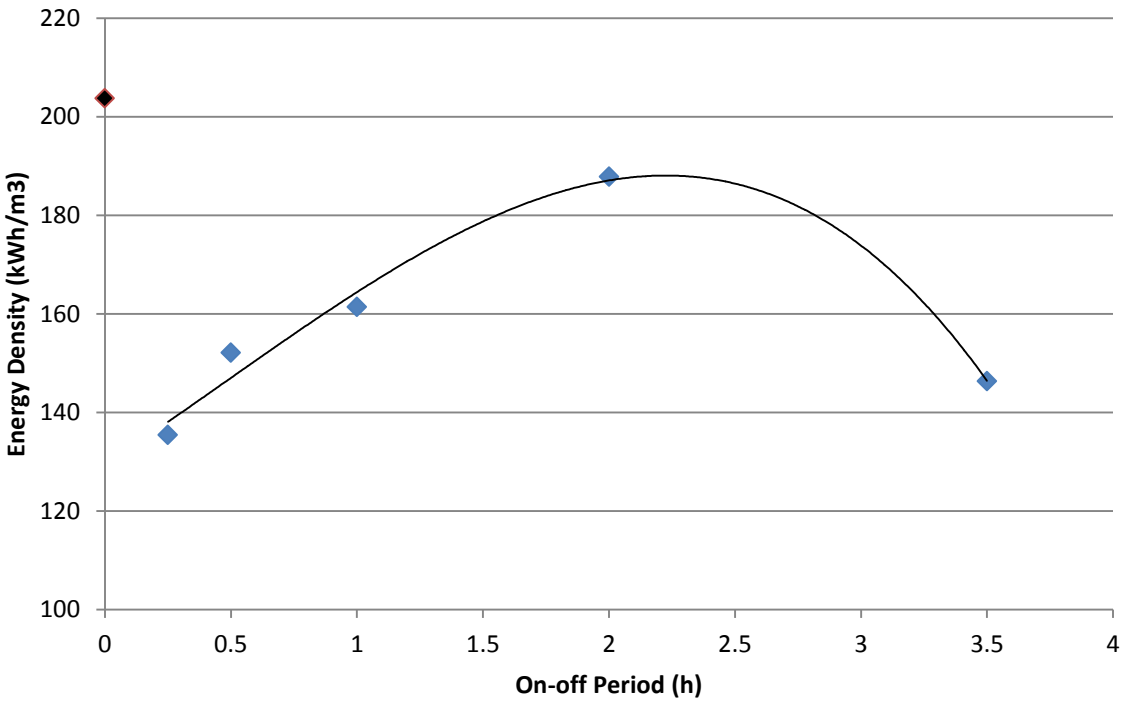

Figure 2.8: Energy density versus on-off periods done during the adsorption run at 30 L/min flow rate for 1 L column with adsorbent 4

Figure 2.9 shows the breakthrough curve with respect to time for an on-off experiment for adsorbent 4, which is done with 2 hours of on-off periods, at 30 L/min flow rate, and with an inlet air relative humidity of 100%. Figure 2.10 shows the outlet and inlet air temperatures with respect to time for the same experiment. Only the on periods that humid air is passing through the column are plotted on both graphs, and as seen from the both figures, every time the column is reopened, adsorption process continues from the point where it is left showing that isolating the adsorption column for 2 hours is not long enough for the complete dissipation and diffusion of the adsorbed water through the column. Furthermore, in on-off experiments, column saturation occurs earlier than regular adsorption runs. This saturation time difference occurs as the adsorbed water particles dissipate through the adsorbent bed during off periods.

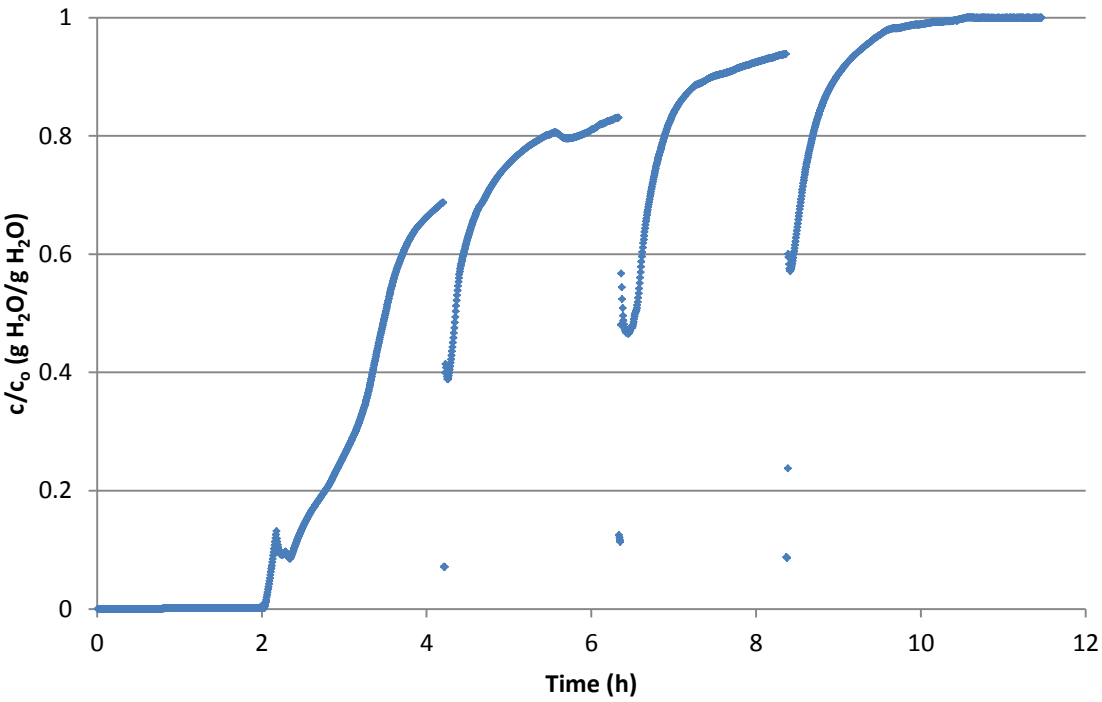

Figure 2.9: Breakthrough curve for on-off adsorption with adsorbent 4 for time period of 2 hours, at 30 L/min flow rate for 1 L column (only adsorption periods are shown)

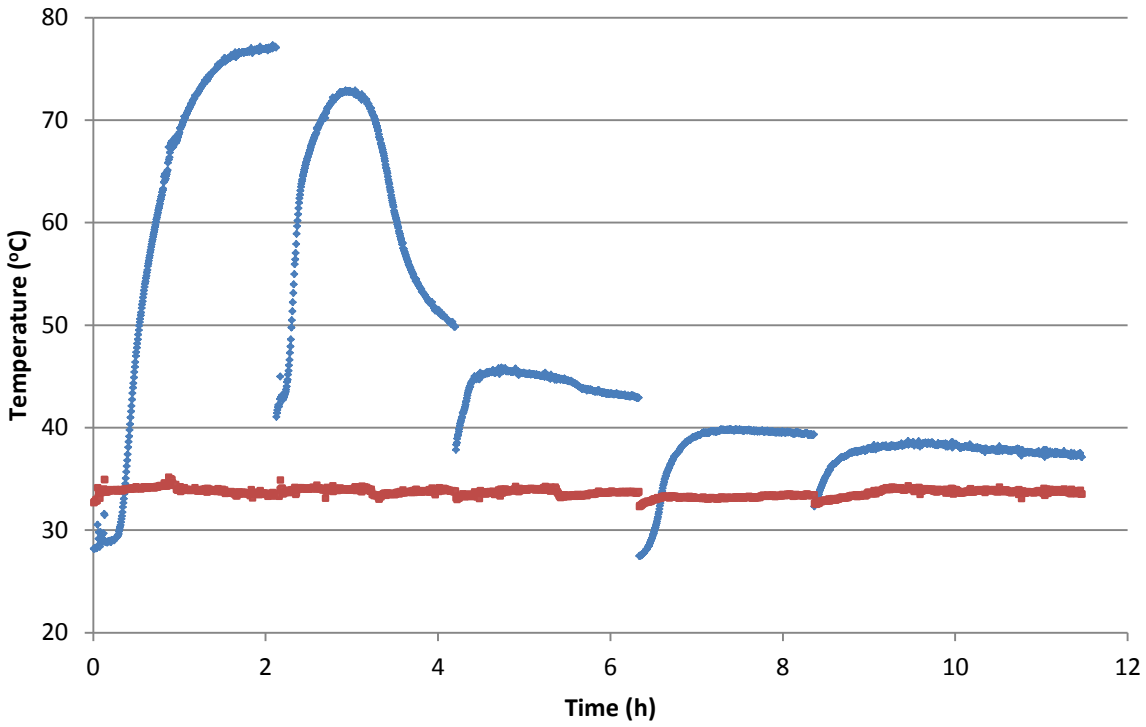

Figure 2.10: Outlet and inlet temperatures with respect to time for on-off adsorption with adsorbent 4 for time period of 2 hours, at 30 L/min flow rate for 1 L column (only adsorption periods are shown)

2.4 Conclusions

Previous work done for thermal energy storage system in adsorbent beds is firstly confirmed. Then, adsorbent screening is performed with various hybrid adsorbent compositions, and energy density is increased up to 226.1 kWh/m^3. Moreover, feasibility of this system for a larger scale column is confirmed by obtaining a similar energy density value after replacing the existing column with 16 times bigger one which has a volume of 1 L. Moreover, on-off experiments are performed on 1 L column in order to investigate the applicability of releasing the stored thermal energy step by step instead of releasing all at once. Even the final obtained energy density and the adsorption capacity decreases, the system is still more efficient than many other thermal energy storage systems as it gives a higher energy density and gives the opportunity of releasing thermal energy whenever it is required and as much as it is needed.

2.5 References

Abedin, A. H., Rosen, M. A. (2011). "A Critical Review of Thermochemical Energy Storage Systems". The Open Renewable Energy Journal, 4, 42-46.

Breck, D. W. (1974) "Zeolite Molecular Sieves Structure, Chemistry and Use". John Wiley & Sons Inc., US.

Dicaire, D. N., Tezel, H. F. (2011) "Regeneration and efficiency characterization of hybrid adsorbent for thermal energy storage of excess and solar heat". Renewable Energy, 36, 3, 986-992.

Duncan, R. (2009). "The City of Austin Energy Depletion Risks Task Force Report". Austin Energy, Texas, U.S.

Geankoplis, C. J. (2003). "Transport Processes and Separation Process Principles". Prentice Hall, New Jersey, U.S.

Hasnain, S. M. (1998). "Review on sustainable thermal energy storage technologies, Part l: heat storage material and techniques". Energy Conversion and Management, 3, 11, 1127-1138.

Hauer, A. (2002). "Thermal energy storage with zeolite for heating and cooling applications." Proceedings of the 7th International Sorption Heat Pump Conference ISHPC, 385-390, Shanghai.

Hendriksen, B. A., Pearce, D. R., Rudham, R. (1972) “Heats of Adsorption of Water on α- and γ-Alumina”. Journal of Catalysis, 24, 82-87.

Hoshi, A., Mills, D. R., Bittar, A., Saitoh, T. S. (2005). ‘Screening of high melting point phase change materials (PCM) in solar thermal concentrating technology based on CLFR”. Solar Energy, 79, 332-339.

International Energy Agency, Energy Conservation through Energy Storage Programme, March 2006. Downloaded on March 27, 2013 from http://www.iea-eces.org/files/brochure06.pdf

Janchen, J., Stach, H. (2012) “Adsorption properties of porous materials for solar thermal energy storage and heat pump applications”. Energy Procedia, 30, 289-293.

Johansson, T. B., Kelly, H., Reddy, A. K. N., Williams, R. (1993). "Renewable Energy Sources for Fuels and Electricity”. Island Press, Washington, D.C.

Kim, J., Lee, C. (2003). “Adsorption Equilibria of Water Vapor on Alumina, Zeolite 13X, and Zeolite X/Activated Carbon Composite”. J. Chem. Eng. Data, 48 (1), 137-141.

3. Modeling of Water Vapor Adsorption from Ambient Air with Hybrid Adsorbent of Activated Alumina and Zeolite

ABSTRACT

In this chapter, water vapor adsorption process from ambient air by using hybrid adsorbent of activated alumina and zeolite is modeled by using Wolfram Mathematica. This modeling is done by performing mass balance in the column, adsorbed water accumulation balance in the pellet, energy balance in the column, and energy balance around the column wall. Comparison between the modeled and experimental results show that the model estimates breakthrough time, and energy density with 98% and 96% accuracy, respectively. Also, this estimation obtained both for two columns with different sizes to show that this model can be used in analyzing, and designing commercial size adsorption columns at different volumes. Due to the assumptions of negligible adsorbent resistance for adsorption and instant adsorption at the pellet surface, a difference between the saturation times of modeled and experimental data occurs at high flow rates. Because of the same assumptions, there is also a difference between the modeled and experimental temperature versus time graphs as the modeled outlet column temperature reaches a higher maximum, and decreases immediately while the experimental data reaches a lower maximum, and decreases slowly.

3.1 Introduction

In Canada, 70% of the energy used in residential, industrial, and commercial buildings is used as thermal energy (for heating and hot water) [Natural Resources Canada, 2013]. Increasing public concern about the environmental impacts of fossil fuels drives us to explore new sources such as renewable and clean energy. The biggest disadvantage of renewable energy is its high cost compared to fossil fuels. However, as resources become depleted and prices for standard commodities, like oil, keep rising, clean and sustainable technologies can become more attractive and economically feasible [Dicaire and Tezel, 2011].

Thermal energy storage in adsorbent beds is one of the emerging renewable energy processes. In this method, instead of obtaining thermal energy from conventional sources, like fossil fuels, it is collected from unconventional sources, like solar radiation and/or power plants that have excess thermal energy. This collected thermal energy is stored in adsorbent beds during regeneration run and can be released by performing exothermic adsorption process of water vapor from air to heat the flowing air when it is required. This heated air can then be used for space or water tank heating. The main advantage of this system is that it allows energy storage without any depletion during the storage period so that it can be stored as long as it is required [Abedin and Rosen, 2011].

Adsorption process is mainly occurs in three steps. Firstly, adsorbate molecules are transferred through the bulk fluid to the surface of the adsorbent. Then, they diffuse into the pores of the adsorbent, and finally, they are adsorbed on the surface of the pores.

Adsorption can be explained by using mass and heat transfer phenomena, and the surface interaction between adsorbates and active sites of the adsorbent [Chou, 1987].

The main objective of this chapter is to model the exothermic adsorption of water vapor from air in Wolfram Mathematica programming environment in order to estimate the breakthrough time and curve, energy density, and the temperature profile of any water vapor adsorption system at different column volumes and at different volumetric flow rates. This modeling is done by using macro pore properties of the adsorbent, and physical properties of gas stream (air) with changing temperature and humidity.

3.2 Experimental Setup

The schematic diagram of the process is given in Figure 3.1. Similar experimental procedure that is explained in Section 2.2 – Experimental Setup is used. In adsorption process, firstly, entering air is filtered by passing it through an air filter in order to separate the undesired particulates such as dust. Then, it is humidified up to 97% relative humidity in the bubbler. Water level of the bubbler is stabilized by supplying water with water pump. This humid air then enters into water trap where water droplets are removed from the flowing humid air. Finally, air passes through the adsorption column where water vapor adsorption from air is carried out by using a hybrid adsorbent of activated alumina and zeolite. Dry and warm air (which can reach up to 78^{o}C) is obtained at the exit of the adsorption column. This warm air can then be used for space heating. Humidity of the exiting air from the column increases gradually as time passes due to the saturation of the adsorbents (due to the breaking through of the adsorbate water vapor from the column).

In regeneration process, air again is passed through the air filter. After filtering, it is heated with an in-line heater to 250^{o}C. In literature, this temperature is found to be the most efficient regeneration temperature to obtain a higher energy density [Dicaire and Tezel, 2011]. In real-time applications of this technology, the heat necessary to heat up the air to 250^{o}C will be provided by solar energy or by waste heat. This heated air is then passed through the adsorption column to regenerate the adsorbents by releasing (evaporating) the water from the adsorbent pores. Humidity of the air exiting the column is measured continuously in both processes in order to monitor the outlet humidity with respect to time. Before measuring the outlet relative humidity, air is passed through a cooling coil in order to ensure a humidity reading at constant temperature. Temperatures with respect to time graphs are obtained at the column inlet and outlet, and at different positions on the column. Those temperature values are measured by thermocouples supplied from Omega. Calibration of the rotameters 1 and 2 are done by using Wet Test Meter.

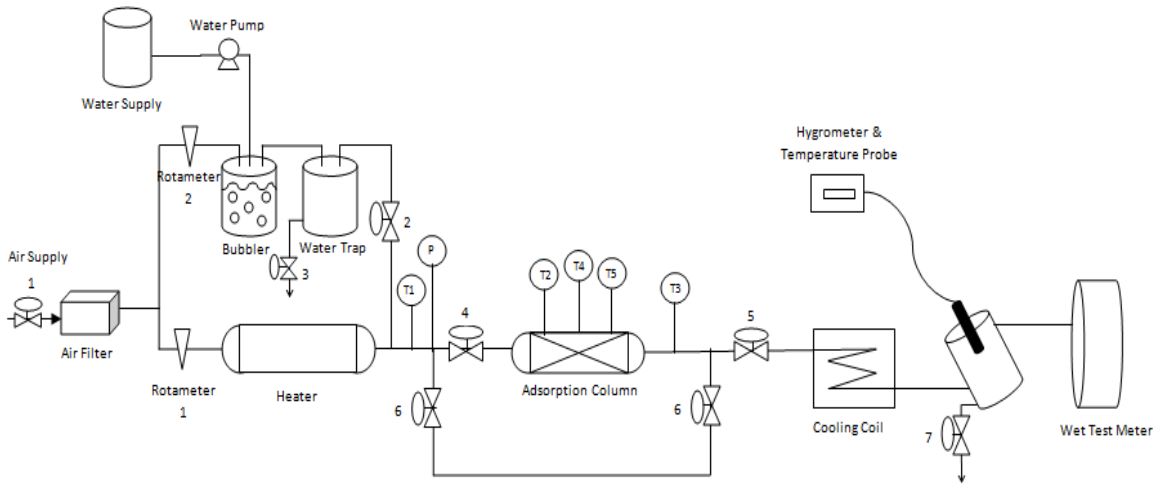

Figure 3.1: Schematic diagram of the experimental setup

Same experimental setup that is explained in Section 2.2 – Experimental Setup is used while conducting the experiments. Air is supplied from the building's compressor. Two rotameters are used: rotameter 1 is used to control the dry air flow during regeneration, and rotameter 2 is used to control the humid air flow during adsorption. 1/4" tubing is used in the setup. Silicone is used for the parts around room temperature, and stainless steel tubing is used for the parts at high temperatures. Two adsorption columns are used: small (volume of 62.76 mL, L/D ratio of 1.8) and big (volume of 1 L, L/D ratio of 2.8). Both columns are made out of stainless steel 314 and are welded with 1/4" pipes at the column entrance and exit. Both of columns are filled with hybrid adsorbent of activated alumina and zeolite with alkaline treatment (adsorbent 2 mentioned in Chapter 2). In the bubbler, humidification is done by using a Hagen Exo Terra Ultrasonic Fog Generator which sits in around 8 centimeters of water. In-line heater (AHP-5051) that is used in regeneration is connected to a rheostat which is used to stabilize the temperature of the flowing air. Relative humidity measurements are done by a hygrometer (HX-15W) which is composed of high temperature and relative humidity sensors and a transmitter. It is supplied from Omega.

3.3 Model Description of the Adsorption Process

Water vapor adsorption is modeled both for 62.76 mL and 1 L adsorption columns. Modeling is done by doing a mass balance in the column, an adsorbed water balance in the pellets, an energy balance in the column, and finally an energy balance around the column wall. Assumptions made before modeling the process are mentioned in Table 3.1.

Table 3.1: Simplifying assumptions made for the modeling

• Constant void fraction throughout the column
• Constant void fraction for every pellet
• Constant gas stream and superficial velocity
• Physical properties of zeolite are applicable to hybrid adsorbent
• Adsorption equilibrium data for zeolite is applicable to hybrid adsorbent
• Working gas stream is taken as ideal gas
• Negligible pressure drop through the column
• No insulation around the column
• Negligible adsorbent resistance for adsorption
• Instantaneous adsorption at the pellet surface
• No radial change in concentration and temperature in the column

Physical properties of the gas stream (humid air) flowing through the column are calculated for changing temperature, humidity (water vapor content), and pressure of the stream. Equations are derived from Perry's Chemical Engineers' Handbook [Perry and Green, 2008] and are used to calculate humidity of the gas stream, partial pressure of the water vapor in the stream, density of the gas stream, heat capacities of the pure air, pure water vapor and gas stream, respectively.

$$T = \frac{T_{inlet} + T_{outlet}}{2} \tag{3.1}$$

$$Y = \left(\frac{RH\%}{100}\right) \times 0.0042 \times e^{(0.0629 \times (T - 273.15))} \tag{3.2}$$

$$p = \frac{Ppa \times Y}{\left(\frac{M_w}{M_a}\right) + Y} \tag{3.3}$$

$$\rho_g = \frac{Ppa - (0.378 \times p)}{287.1 \times T} \tag{3.4}$$

$$c_{pa} = (a_a + b_a T + c_a T^2 + d_a T^3) / MW_a \tag{3.5}$$

$$c_{pw} = (a_w + b_w T + c_w T^2 + d_w T^3) / MW_w \tag{3.6}$$

$$c_{pg} = c_{pa} + (c_{pw} \times Y) \tag{3.7}$$

Axial dispersion coefficient (D_Z) and mass transfer coefficient (k_G) of water in the gas stream are calculated by using the following equations. Both coefficients are estimated by using molecular diffusivity, Reynolds, and Schmidt numbers which are calculated using physical properties of the gas stream [Incropera et al., 2007; Wakao and Funazkri, 1978].

$$\mathrm{Re}_p = \frac{\rho_g v_g D_p}{\mu_g} \tag{3.8}$$

$$Sc = \frac{\mu_g}{\rho_g D_m} \tag{3.9}$$

$$D_z = \frac{D_m}{\varepsilon_c}[20 + 0.5(\mathrm{Re}_p)(Sc)] \tag{3.10}$$

$$k_G = \frac{D_m}{D_p}[2.0 + 1.1(\mathrm{Re}_p)^{0.6}(Sc)^{0.33}] \tag{3.11}$$

Heat transfer coefficient of the gas phase in the column and the heat transfer coefficient of the ambient air outside of the column are estimated to be used in energy balances. They are estimated by using the following equations which use Nusselt, Rayleigh, Prandtl numbers, and physical properties of the gas stream in the column (denoted by subscript g) as well as the physical properties of the surrounding air (denoted by subscript a) [Churchill and Chu, 1975; Incropera et al., 2007].

$$\nu_{a,g} = \frac{\mu_{a,g}}{\rho_{a,g}} \tag{3.12}$$

$$\mathrm{Pr}_{a,g} = \frac{c_{pa,g}\mu_{a,g}}{k_{a,g}} \tag{3.13}$$

$$Ra = \frac{\beta \Delta T g D^3 \,\mathrm{Pr}}{\nu^2} \tag{3.14}$$

$$Nu = \left(0.60 + \frac{0.387(Ra)^{1/6}}{[1+(\frac{0.559}{\mathrm{Pr}})^{9/16}]^{8/27}} \right)^2 \tag{3.15}$$

$$h_o = \frac{k_a Nu_a}{D_o} \tag{3.16}$$

$$h_{fD} = \frac{k_g Nu_g}{D_i} \tag{3.17}$$

Average thermal capacity of the gas stream is estimated for energy calculations. This estimation is done by using physical properties of the gas stream and the pellet [Hashi et al., 2010].

$$\eta = \rho_g c_{pg}[\varepsilon_c + (1-\varepsilon_c)\varepsilon_p] + [(1-\varepsilon_c)(1-\varepsilon_p)\rho_p c_{pp}] \tag{3.18}$$

Finally, equilibrium concentration value that is used in mass balances is calculated from Temperature Dependent Toth Isotherm. This isotherm is used as it is valid for the adsorption processes with varying temperatures and pressures in a wide range [Duong, 1998]. A relationship between the adsorbed water amount and the water concentration in the gas phase is set by using ideal gas law and Temperature Dependent Toth Isotherm which are shown in equations below, respectively [Wang and LeVan, 2009].

$$p = c_{ge} RT \tag{3.19}$$

$$q = \frac{ap}{\left[1 + (bp)^n\right]^{1/n}} \tag{3.20}$$

where $a = a_0 exp\left(E/T_g\right)$ (3.21)

$$b = b_0 exp\left(E/T_g\right) \tag{3.22}$$

$$n = n_0 + c/T_g \tag{3.23}$$

Table 3.2: Temperature-dependent parameters of the Toth Isotherm Model for water vapor adsorption with zeolite 13X [Wang and LeVan, 2009].

$a_o \left(\frac{mol}{kg.kPa} \right)$	3.63×10^{-6}
$b_o \left(\frac{1}{kPa} \right)$	2.41×10^{-7}
$E\ (K)$	6852
n_o	0.3974
$c\ (K)$	-4.199

3.3.1 Mass Balance in the Column

While performing the mass balance around the column, it is assumed that there is an instantaneous equilibrium between the gas stream and the solid adsorbent surface. Therefore, diffusion of the adsorbates inside the particles is not considered. (The rate of diffusion in the pellet is assumed to be very high.) Following equation (equation 3.24) which considers water vapor accumulation in the column, axial diffusion in the column, convection through the column, and mass transfer due to adsorption is used [Hashi et al., 2010].

$$\varepsilon_c \frac{\partial c_g}{\partial t} = \varepsilon_c D_z \frac{\partial^2 c_g}{\partial z^2} - v_g \frac{\partial c_g}{\partial z} - (1-\varepsilon_c)\rho_p \frac{\partial q}{\partial t} \tag{3.24}$$

Mass balance is solved by assuming that water vapor concentration is zero at the beginning of the process, pellets do not contain any adsorbed water initially, gas stream enters the

column with a constant inlet water vapor concentration (at 100% relative humidity), and concentration change with respect to distance is equal to zero at the column exit. Thus, the following initial and boundary conditions are used for the process [Hashi et al., 2010].

$$c_g\Big|_{t=0} = 0 \qquad \text{(for all z and r values)} \tag{3.25}$$

$$c_g\Big|_{z=0} = c_{g,inlet} \qquad \text{(for all r and t values)} \tag{3.26}$$

$$\left.\frac{\partial c_g}{\partial z}\right|_{z=L} = 0 \qquad \text{(for all r and t values)} \tag{3.27}$$

$$q\big|_{t=0} = 0 \qquad \text{(for all z and r values)} \tag{3.28}$$

3.3.2 Adsorbed Water Balance in the Pellet

Adsorbed water amount in the pellet (adsorption term used in equation 3.24) is calculated by deriving the water accumulation rate in the pellet. As we assumed that rate of diffusion in the pellet is very high and there is instant adsorption, accumulation in the pellet is calculated by using the concentration difference between the gas stream in the bulk phase and at the surface of the adsorbed phase (equilibrium phase) [Hashi et al., 2010].

$$(1-\varepsilon_c)\rho_p \frac{\partial q}{\partial t} = k_G\left[\frac{3\cdot\varepsilon_c}{r_p}\right](c_g - c_{ge}) \tag{3.29}$$

For the initial condition, it is assumed that there is no water vapor in the column initially [Hashi et al., 2010].

$$q\big|_{t=0} = 0 \qquad \text{(for all z and r values)} \tag{3.28}$$

3.3.3 Energy Balance in the Column

Temperature of the gas stream (bulk phase in the column) is calculated by doing an energy balance around the column. Energy balance is done by considering the energy accumulation, conduction and convection in the column, heat released due to adsorption (heat of adsorption is determined experimentally), and heat loss from the walls [Hashi et al., 2010; Incropera et al., 2007].

$$\eta \frac{\partial T_g}{\partial t} = k_g \frac{\partial^2 T_g}{\partial z^2} - \varepsilon_c v_g \rho_g c_{pg} \frac{\partial T_g}{\partial z} - \frac{2h_{fD}}{r_c}(T_g - T_w) - \rho_p \Delta H_{ads} \frac{\partial q}{\partial t} \tag{3.30}$$

In order to solve Equation 3.30, we assumed that temperature of the gas stream is equal to the ambient temperature (room temperature) initially, gas stream temperature at the column inlet is equal to the ambient temperature (room temperature), temperature change with respect to column distance is equal to zero at the column exit, and there is no water vapor in the pellets initially. [Hashi et al., 2010; Incropera et al., 2007]

$$T_g\big|_{t=0} = T_o \tag{3.31}$$

$$T_g\big|_{z=0} = T_o \tag{3.32}$$

$$\left.\frac{\partial T_g}{\partial z}\right|_{z=L} = 0 \tag{3.33}$$

$$q\big|_{t=0} = 0 \tag{3.28}$$

3.3.4 Energy Balance around the Column Wall

Wall temperature is used while calculating the temperature of the gas stream. In order to obtain a proper wall temperature value, heat loss from the walls must be considered. Therefore, an energy balance around the walls is done by considering accumulated energy in the walls, convection from walls to gas stream in the column, and convection from walls to surrounding ambient air [Hashi et al., 2010; Incropera et al., 2007].

$$(r_o^2 - r_c^2)\rho_w c_w \frac{\partial T_w}{\partial t} = 2r_c h_{fD}(T_g - T_w) - 2r_o h_o (T_w - T_o) \tag{3.34}$$

Equation 3.34 is solved by assuming that wall temperature is equal to the ambient temperature (room temperature) initially [Hashi et al., 2010; Incropera et al., 2007].

$$T_w\big|_{t=0} = T_o \tag{3.35}$$

3.3.5 Model Accuracy

After modeling water vapor adsorption process in Mathematica, obtained results are compared with the experimental results in order to estimate the accuracy of the model. This accuracy calculation is done for the breakthrough time and energy density estimations of the model by using the following equation.

$$Accuracy = \frac{ModeledData - ExperimentalData}{ExperimentalData} \times 100 \tag{3.36}$$

3.4 Results and Discussion

The combined mass and energy balances are solved numerically by using method of lines technique in Mathematica. Model and experimental results are compared for the both columns at different volumetric flow rates.

Breakthrough curves shown in Figures 3.2 and 3.3 are obtained for the small and larger columns at different volumetric flow rates, respectively. The model estimates the breakthrough time with 98% accuracy. As seen from the graphs, as the flow rate increases, the difference between the column saturation time of the model and the experimental results increases. This difference occurs as we assumed that there is instant adsorption between the gas phase and pellet surface, and the rate of diffusion of water in the particles to be very high. Therefore, as the model assumes there is no pellet resistance and there is instant adsorption, it estimates that as the flow rate increases, more water molecules passes through the column per time, and more water molecules are adsorbed in the pellets per time. Thus, model predicts that as flow rate increases, saturation time of the column decreases. However, in real time processes, rate of diffusion of water particles in the pellets is not very high. Thus, water molecules need some time to be adsorbed in the pellets. As flow rate increases, residence time of the water molecules in the column decreases and water molecules do not have enough time to be adsorbed in the particles. As a result, saturation time of the column increases as flow rate increases in real time processes as can be seen from Figures 3.2 and 3.3.

Moreover, Figure 3.3 shows the breakthrough curves for 16 times bigger column at different volumetric flow rates for adsorbent 2 mentioned in Chapter 2. As seen from this figure, as flow rate increases, tail end of the breakthrough curves gets more sluggish. This happens due to the enlargement of the mass transfer zone as water molecules have smaller residence time to come to equilibrium at higher flow-rates. Mass transfer zone can be simply defined as the place where adsorption happens in a packed bed reactor. As the adsorbents at the entrance of the reactor get saturated, mass transfer zone moves further along the column [Geankoplis, 2003]. As volumetric flow rate of the gas stream increases, mass transfer zone of the column expands and constitutes the whole column, therefore, the beginning of the breakthrough curve becomes sluggish (see Figure 3.3).

Furthermore, volumetric flow rate ranges for both small and 16 times bigger columns are selected due to the optimum flow rate results obtained in Chapter 2, and experimental results explained in Chapter 2 are compared with the modeled data.

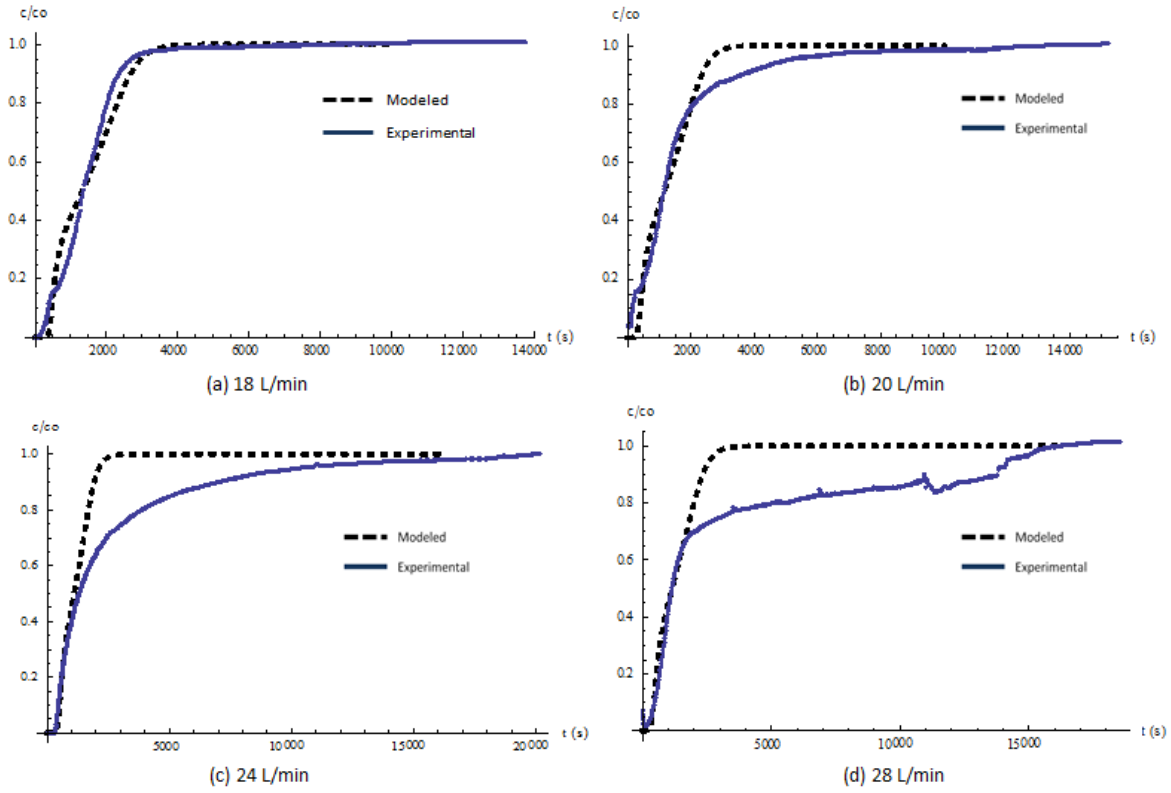

Figure 3.2: Breakthrough curves for 62.76 mL column at different volumetric flow rates

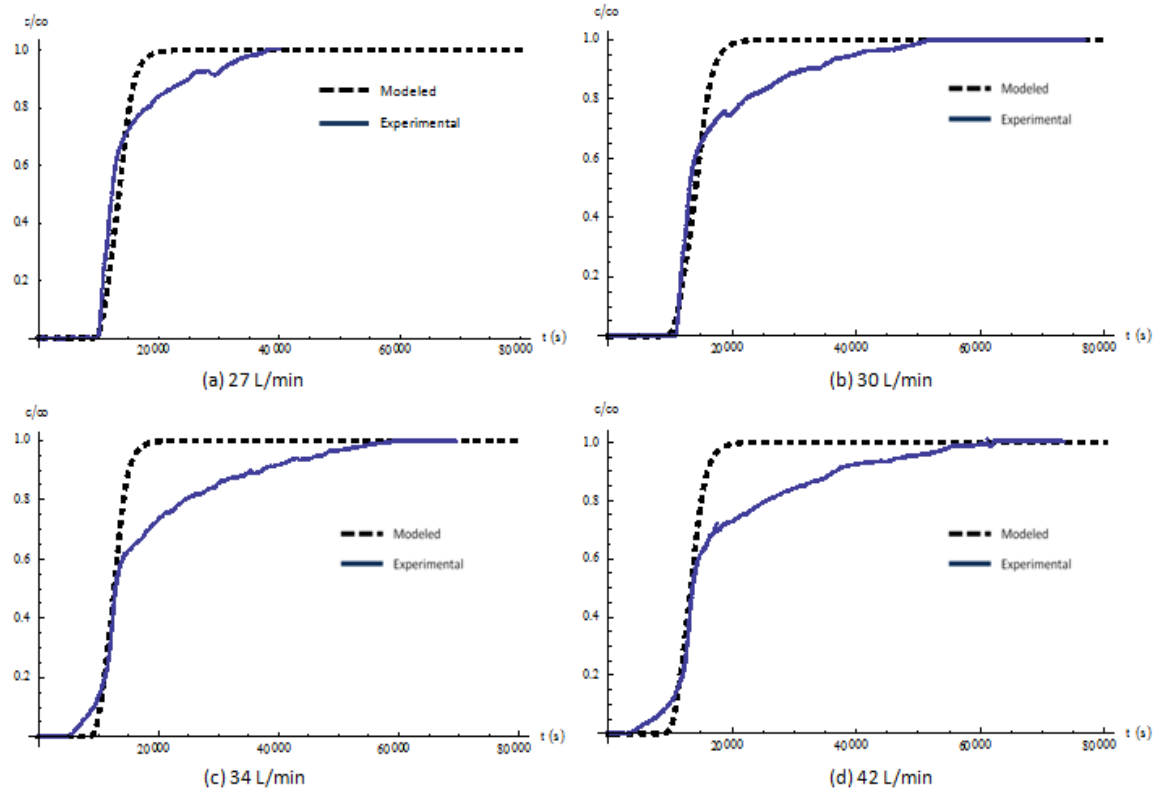

Figure 3.3: Breakthrough curves for 1 L column at different flow rates

From the energy balances, column outlet temperature with respect to time graphs are obtained for both columns, and compared with the experimental results which are shown in figures 3.4 and 3.5. A difference between the model prediction and the experimental results occurs due to the instant adsorption and negligible pellet resistance assumptions. Because of those assumptions, model neglects the required time needed for water molecules to be adsorbed in the pellets. Thus, as seen from Figures 3.2 and 3.3, model predicts that adsorption of water molecules will occur at a constant rate (slope) and finish immediately. Therefore, in models' temperature versus time graph predictions, temperature of the column outlet increases rapidly to higher maximum temperatures than

experimental results, and as the column saturates faster, temperature decrease occurs suddenly. However, in real time processes, water molecules need some time to be adsorbed in the pellet. Therefore, outlet column temperatures cannot reach high maximum temperatures, and as bed saturation does not occur immediately, decrease in the column outlet temperature occurs gradually.

By using the temperature difference between the column inlet and outlet, flow rate, heat capacity and density of the gas stream, and the column volume, energy density is calculated both for the modeled and experimental results. The model estimates the energy density with a 96% accuracy as the extra area that occurs because of the models' higher maximum temperature reach is compensated with the slow temperature decrease of the experimental results.

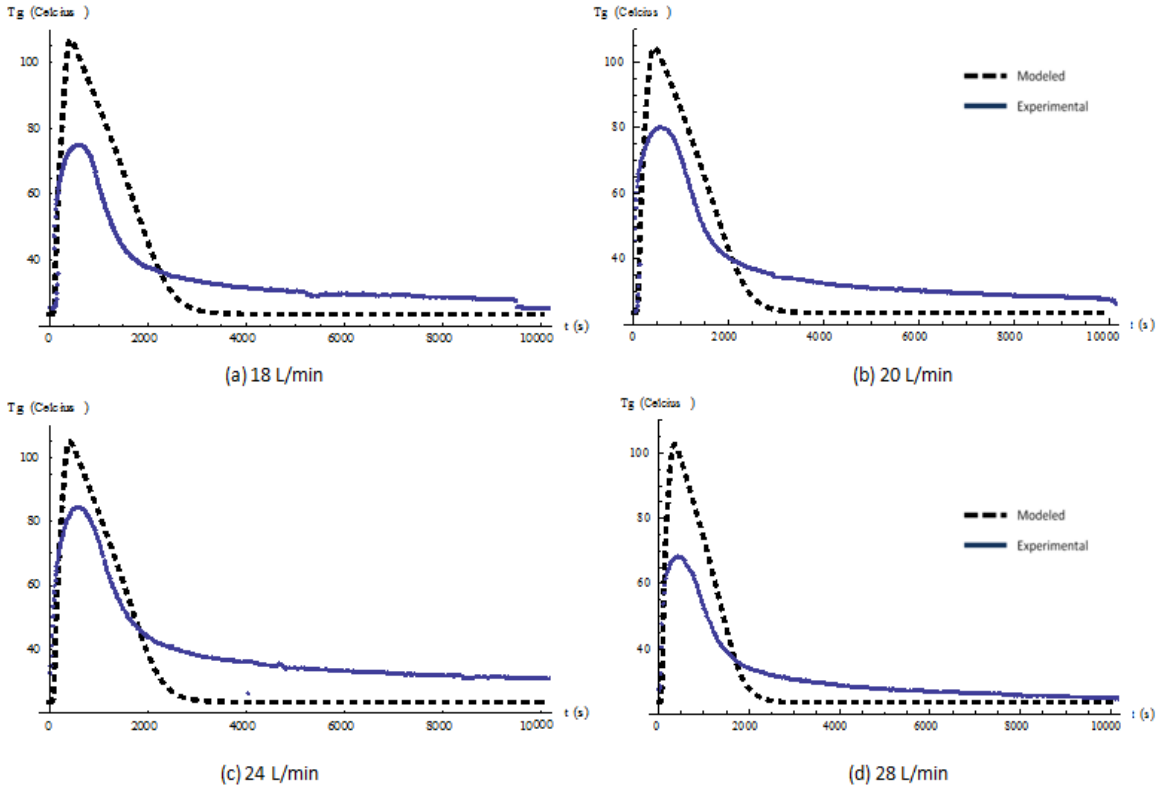

Figure 3.4: Outlet column temperature with respect to time graphs for 62.76 mL column at different volumetric flow rates

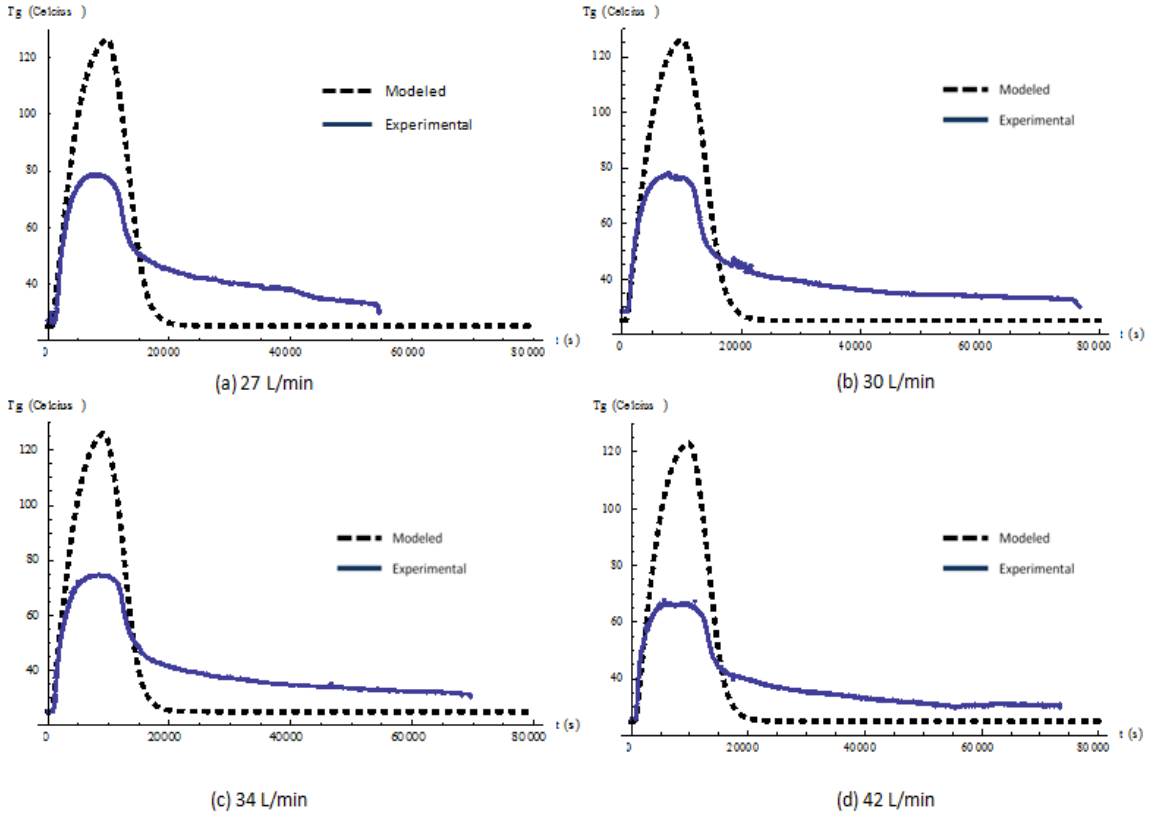

Figure 3.5: Outlet column temperature profile for 1 L column at different volumetric flow rates

3.5 Conclusions

In this chapter, a mathematical modeling of the water vapor adsorption process from ambient air by using hybrid adsorbent of activated alumina and zeolite is explained. This modeling is done by performing mass and energy balances in the column, water accumulation balance in the pellet, and energy balance around the column wall. Then, modeled results are compared with experimental results for two different columns with different volumes, and at different volumetric flow rates. This comparison shows that modeled results are in a good agreement with the experimental data as it estimates the breakthrough time, and energy density with high accuracy. Also, obtaining the same accuracy for the 16 times bigger column proves that this model can be used for energy density, and breakthrough time estimations for bigger, commercial size adsorption columns. The only differences between the model and the experimental data are the difference between the saturation times at high volumetric flow rates, maximum temperature reached, and the rate of the temperature decrease with respect to time. These differences are caused due to the neglection of the adsorbent resistance to adsorption and assumption that there is an instant adsorption. However, they can be eliminated by performing an additional mass balance around the particles considering the rate of water vapor diffusion in the pores.

3.6 Nomenclature

Constants	*Definition*	*Value*	*Unit*
a_a	Parameter of heat capacity calculation	28.088	J/mol.K
a_w	Parameter of heat capacity calculation	32.218	J/mol.K
b_a	Parameter of heat capacity calculation	0.00192	$J/mol.K^2$
b_w	Parameter of heat capacity calculation	0.00192	$J/mol.K^2$
c_a	Parameter of heat capacity calculation	$0.48x10^{-5}$	$J/mol.K^3$
c_w	Parameter of heat capacity calculation	$1.055x10^{-5}$	$J/mol.K^3$
c_g	Water concentration in the gas phase	-	mol H_2O/m^3air
c_{ge}	Equilibrium water concentration in the gas	-	mol/m^3
c_{pa}	Heat capacity of air	-	J/kg.K
c_{pg}	Heat capacity of the gas stream	-	J/kg.K
c_{pp}	Heat capacity of the pellet	836.8	J/kg.K
c_{pw}	Heat capacity of water vapor	-	J/kg.K
c_w	Heat capacity of the column wall	473	J/kg.K
d_a	Parameter of heat capacity calculation	$-1.965x10^{-9}$	$J/mol.K^4$
d_w	Parameter of heat capacity calculation	$-3.593x10^{-9}$	$J/mol.K^4$
D	Diameter	0.0381, 0.088	m
D_i	Inside diameter of the column	0.03391, 0.078	m
D_m	Molecular diffusivity	$0.27x10^{-2}$	m^2/s
D_p	Diameter of the pellet	0.0023	m
D_z	Axial dispersion	-	m^2/s
g	Gravitational accelaration	9.8	m/s^2
H_{ads}	Heat of adsorption	42 000	J/mol
h_{fD}	Heat transfer coefficient in the bulk phase	-	$W/m^2.K$
h_o	Heat transfer coefficient in the outside	-	$W/m^2.K$
k_g	Thermal conductivity of the gas stream	0.0263	W/m.K
k_G	Mass transfer coefficient	-	m/s
k	Thermal conductivity of the vapour mixture	0.4	W/m.K
L	Column length	0.0695, 0.189	m
M_a	Molar mass of air	28.97	g/mol
M_w	Molar mass of water	18.01	g/mol
Nu	Nusselt number	-	Dimensionless
Nu_a	Nusselt number for ambient air	-	Dimensionless
Nu_g	Nusselt number for the gas stream	-	Dimensionless
p	Water vapor partial pressure	-	Pa

Ppa	Column pressure	-	Pa
Pr	Prandt number	-	Dimensionless
Pr_a	Prandt number for the ambient air	-	Dimensionless
Pr_g	Prandt number for the gas stream	-	Dimensionless
q	Adsorbed water in the pellet	-	mol H_2O/kg pellet
Re_p	Reynolds number for the particles	-	Dimensionless
Sc	Schmidt number	-	Dimensionless
r_c	Inside radius of the column	0.01695, 0.039	m
r_o	Outer radius of the column	0.01905, 0.044	m
r_p	Pellet radius	0.00115	m
RH%	Relative Humidity	0-100	%
t	Time	-	s
T	Average temperature	-	K
T_g	Temperature of the gas stream	-	K
T_{inlet}	Inlet gas stream temperature	298.15	K
T_{outlet}	Outlet gas stream temperature	-	K
T_o	Ambient air temperature	298.15	K
T_w	Temperature of the wall	-	K
v_g	Superficial velocity of the fluid	-	m/s
Y	Humidity	-	kg H_2O/kg dry air

Greek Constants	*Definition*	*Value*	*Unit*
ε_c	Void fraction of the column	0.39	m^3 void/m^3 column
ε_p	Void fraction within the pellet	0.4695	m^3 void/m^3 column
Δ	Difference	-	Dimensionless
μ_g	Gas stream viscosity	-	kg/m.s
ρ_g	Density of the gas stream	-	kg/m^3
ρ_p	Bulk density of the pellet	1061	kg/m^3
ρ_s	Solid density of the pellet	2000	kg/m^3
ρ_w	Density of the column wall	8238	kg/m^3
ν_g	Kinematic viscosity of gas stream	-	m^2/s
ν_a	Kinematic viscosity of ambient air	0.00001589	m^2/s

3.7 References

Abedin, A. H., Rosen, M. A. (2011). “A Critical Review of Thermochemical Energy Storage Systems”. The Open Renewable Energy Journal, 4, 42-46.

Chou, C. L. (1987) “Dynamic Modelling of Water Vapor Adsorption by Activated Alumina” Chemical Engineering Communications, 56:1-6, 211-227

Churchill, S.W., Chu, H. H. S. (1975) “ Correlating Equations for Laminar and Turbulent Free Convection from a Horizontal Cylinder” Int. J. Heat Mass Trans., 18, 1049-1053.

Dicaire, D. N., and Tezel, H. F. (2011) “Regeneration and efficiency characterization of hybrid adsorbent for thermal energy storage of excess and solar heat”. Renewable Energy, 36, 3, 986-992.

Duong, D. D. (1998). “Adsorption analysis: equilibria and kinetics”. Imperial College Press, London.

Geankoplis, C. J. (2003). “Transport Processes and Separation Process Principles”. Prentice Hall, New Jersey, U.S.

Hashi, M., Thibault, J., Tezel, F.H., (2010) “Recovery of ethanol from carbon dioxide stripped vapour mixture: adsorption predicting and modeling,” Ind. Eng. Chem. Res. 49, 8733–8740.

Incropera, F.P., Dewitt, D.P., Bergman, T.L., Lavine, A.S. (2007) “Introduction to Heat Transfer”. Wiley, New Jersey.

Natural Resources Canada. Renewables: Solar-Thermal. Retrieved on March 15, 2013 from http://canmetenergy-canmetenergie.nrcan-rncan.gc.ca/eng/renewables/solar_thermal.html

Perry, R. H., Green, D. W. (2008) "Perry's Chemical Engineers' Handbook". McGraw-Hill, New York.

Wakao, N., Funazkri, T., (1978) "Effect of fluid dispersion coefficients on particle-to-fluid mass transfer coefficients in packed beds: correlation of Sherwood numbers," Chem. Eng.. Sci., 33, 1375-1384

Wang, Y., LeVan, M. D. (2009). "Adsorption Equilibrium of Carbon Dioxide and Water Vapor on Zeolites 5A and 13X and Silica Gel: Pure Components". J. Chem. Eng. Data, 54, 2839-2844.

4. Plant Design and Economic Analysis of Thermal Energy Storage System in Adsorbent Beds

ABSTRACT

In this chapter, plant design and economic analysis of thermal energy storage system in adsorbent beds are performed. In order to obtain a more realistic economic analysis results, plant design is conducted for power plant application of this process in which a thermal energy storage system is installed next to an existing power plant to store its excess, low quality thermal energy obtained from turbine outlet. Firstly, thermal energy storage plant layout is shown, process is reviewed, and the design of the equipments used in the process is explained. Then, the calculation of purchase equipment cost, total capital investment, and annual production cost are explained in detail for the 100 MWh/year thermal energy storage plant. (All cost estimations are done for the year of 2013.) By assuming a 15-year payback period, thermal energy price is also calculated for this plant. Finally, cost estimations are done for different storage capacities, and thermal energy price is calculated for those storage capacities by assuming different payback periods.

For 100 MWh/year storage plant, purchased equipment cost is found as $119,300. Total capital investment is calculated as $777,150 by using the adsorbent cost required to fill the column, purchased equipment cost value, and the ratios of it. Annual production cost is calculated as $53,650/year from the costs of labor, utility, patents, and etc. Thermal energy price is calculated for two cases: (i) regular case where total capital investment is taken as initial investment, and (ii) bare bone case where purchased equipment cost and adsorbent cost are taken as initial investment. For 15 years of payback period, thermal energy price is calculated as $1.055/kWh for the regular and $0.716/kWh for the bare bone case.

These purchased equipment cost, total capital investment, annual production cost, and thermal energy price estimations are also done for different thermal energy storage capacities and payback periods. It is found that thermal energy price decreases with increasing storage capacity and payback period.

Most of the clean or renewable energy production plants are supported by the government in many countries (especially in Canada). Thus, it is highly possible that our plant also receives a government funding. After making a detailed comparison between the projects which earned the Clean Energy funding from Canadian Government, a yearly budget amount is estimated for each storage capacity. Then, thermal energy prices are recalculated and it is found that with the help of the funding, thermal energy price can be lower than the commercial electricity prices of many countries.

4.1 Introduction

Thermal energy is a basic requirement for all industrial, commercial, and residential operations. Currently, majority of this required thermal energy is obtained from conventional sources, like fossil fuels. However, with growing impact of fossil fuels on health and environment, rising prices, and depletion risk of fossil fuel sources, attention has been drawn to renewable energy technologies [Duncan, 2009]. Thermal energy storage system in adsorbent beds is one of those resulting technologies.

Thermal energy storage in adsorbent beds is a thermo-chemical storage method in which exothermic adsorption and endothermic regeneration processes are used. In this system, regeneration energy, which is used to reactivate the adsorbent, is stored. When the thermal energy is needed, exothermic adsorption process is carried out to release the stored energy. Water vapor adsorption from ambient air is selected to be used in this system due to being costless and safe raw materials. In literature, optimum conditions for this process which gives the highest energy density are found as using inlet air at 100% relative humidity, regenerating at 250^{o}C, and using hybrid adsorbent of activated alumina and zeolite [Dicaire and Tezel, 2011].

There is a wide application range for this process such as storing solar energy and excess heat produced by power plants. In summer months, high amounts of solar energy which meets the thermal energy requirements for the whole year is received. However, solar collectors can only store this received energy for short terms. It must be used within a few days or else it will be lost to the environment. Therefore, adsorbent beds can be used to

store this lost solar energy, and the stored thermal energy can be used in the winter or at nights [Dicaire and Tezel, 2011]. In all power plants, after the fuel combustion, electricity is produced by using combined heat and power units. In those units, hot exhaust from the combustion chamber enters the turbine where electricity is produced. Then, exhaust from turbine (which is around 400^{o}C) goes to a heat exchanger to produce thermal energy. However, roughly one third of this produced thermal energy is excess, and released to the atmosphere [Waste Heat to Power Systems, 2013]. Thus, this excess thermal energy can also be stored in adsorbent beds, and released when it is required [Naik-Dhungel, 2012].

In this chapter, plant design and economic analysis of a thermal energy storage plant in adsorbent beds are carried out in order to obtain a thermal energy price for selling the stored energy. Plant design is carried out for the second application of this system in which excess thermal energy supplied from power plants is stored. This application specification is done in order to conduct more precise plant design and economic analysis of the system.

4.2 Plant Layout and Process Description

Overall plant layout is given in Figure 4.1. During adsorption process, ambient air first enters the air filter in which solid particulates and bacteria are removed. This filtered air then enters the bubbler to increase its relative humidity by using an ultrasonic humidifier. After exiting the bubbler, humidified air enters into a water trap where the condensed water droplets are captured to prevent the liquid from entering the adsorption column. Finally, air at ambient temperature and 100% relative humidity passes through the adsorption column and exits as warm and dehumidified. (Temperature of the outlet air

from the column decreases gradually as the adsorption column gets saturated, and the humidity of the outlet air increases.)

During desorption process, like in the adsorption process, ambient air first passes through the air filter. Then, it enters the heat exchanger and heated to the optimum regeneration temperature of 250^{o}C. Waste heat received from power plants is used as the heat source for this heating process. Heat exchanger's outlet temperature is continuously checked during the process to make sure the air entering the adsorption column is at 250^{o}C. This heated air is passed through the column in order to desorb all the adsorbed water from the saturated adsorbent bed.

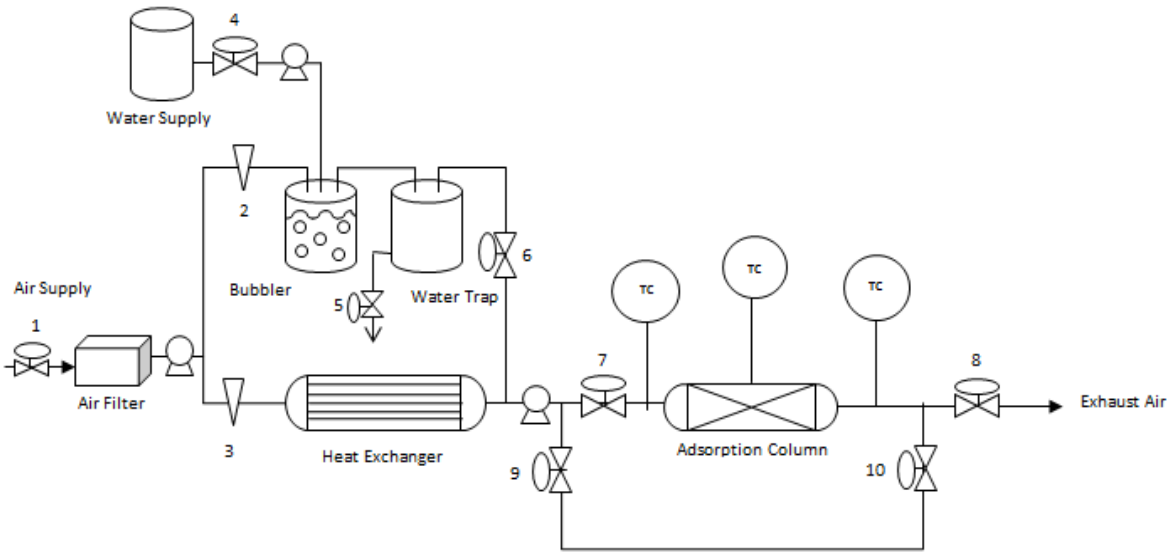

Figure 4.1: Overall Plant Layout

4.3 Selections & Assumptions

Before starting the plant design calculations, some selections and assumptions are made;

- Energy density of the system is 200 kWh/m^3.
- Highest air temperature reached is 75^oC. (Air is heated from 20^oC to 75^oC during adsorption)
- Adsorption column stores 100 MWh of thermal energy per year in total.
- Adsorption column is cylindrical with L/D ratio of 1 to minimize the energy loss from the walls and to minimize the energy required to heat the adsorbents throughout the column until the heated air exits. Column volume is calculated by using the amount of energy stored, and energy density. Column thickness is calculated by using thickness equations in Peters & Timmerhaus [Peters et al., 2003].
- Adsorption column is made out of carbon steel due to its low cost and low thermal conductivity.
- Cotton wool is selected as the insulation material for the column because of its low thermal conductivity. Surface area and the thickness of the cotton wool are calculated by minimizing the heat loss through the walls.
- For the regeneration of the column, shell-and-tube heat exchanger is used due to its low cost, high efficiency and suitability for the process conditions (heating air from 20^oC to 250^oC).
- Air blowers are used as they are the most economically advantageous ones as opposed to centrifugal air pumps due to the range of air flow rate in the process.

- Pipes and valves are designed from the flow rate of the system. Carbon steel screwed valves are used due to their suitable pipe diameter range, low cost, and suitability for the process pressure.
- Bubbler and water trap are designed by extending the bubbler that is used in the experiments. This extension is done by using the same residence time required to humidify the air for bubblers used in experimental setup and designed plant.

4.4 Design of the Process Equipment for 100 MWh/year Storage

Equipments used in the thermal energy storage process are mainly designed by using the volumetric flow rate value. Flow rate is calculated from equation 4.1 by using the average temperature difference between inlet and outlet of the column, average heat capacity of the air passing through the column, and total energy stored in the column per year. Average density, heat capacity and temperature difference values are calculated from the experimental results that are explained in Chapter 2.

$$Q = (\dot{V}.\rho_{av}).c_{p,av}.\Delta T_{av} \quad (4.1)$$

where Q = 100 MWh/year = 3.6×10^8 kJ/year = 11.57 kJ/s

$\dot{V}$ = volumetric flow rate (m^3/s)

ρ_{av} = average density =1.144 kg/m^3

$C_{p,av}$ = average heat capacity = 1.035 kJ/(kg.K)

ΔT_{av} = average temp. difference between column inlet and outlet = 22.5 ^{o}C

Volumetric flow rate of 100 MWh/year energy storage plant is found as 0.501 m^3/s. Equipments that will be used in the process are designed according to this flow rate value. This volumetric flow rate calculation is adjusted when designing plants with different thermal energy storage capacities.

A detailed explanation of the equipment design is given in Appendix 7.2.

4.4.1 Air Filter

Due to volumetric air flow rate of 0.501 m^3/s, the most suitable and economic air filter is found as follows. (HEPA filter has been selected due to its high efficiency in particulate removal.)

Table 4.1: HEPA Air Filter Design Data [HEPA Filters, 2013]

Dimension (mm)	(610x610x149)mm
Maximum Resistance (Pa)	250
Filter Weight (lbs.)	17.0

4.4.2 Adsorption Column

In this process, a cylindrical carbon steel column with L/D ratio of 1 is used to minimize heat loss and the column cost. Column volume is calculated by using the total amount of energy stored (100 MWh/year) and a safety factor of 15% is added. Insulation thickness is determined from a graph of heat loss versus insulation thickness in which heat loss is

minimized for a reasonable insulation thickness. Design data of the adsorption column of the plant is given in Table 4.2. A detailed explanation of these calculations is given in Appendix 7.2.1.

Table 4.2: Design Data for the Adsorption Column with a 100 MWh/year Energy Storage Capacity

Design Values for the Adsorption Column	
Total Volume	575 m^3
Inside Diameter	9.013 m
Length of the column	9.013 m
Wall Thickness	15 mm
Insulation thickness	0.63 m
Outside diameter	10.3 m
Volumetric flow rate	0.501 m^3/s
Energy required for regeneration	97.2 MWh
Heat loss during regeneration	4.04 MWh

4.4.3 Heat Exchanger

Due to low cost and suitability for our system; a shell-and-tube heat exchanger is used. After obtaining the temperature and amount of heat required for regeneration, it is decided to use VOR.CC6360 Heat Exchanger supplied from ITW Vortec [Vortec Products Price List, 2008].

4.4.4 Pipes

By using volumetric flow rate for 100 MWh storage and air viscosity, pipe diameter is found for stainless steel pipes [Peters et al., 2003].

Inside pipe diameter = D_i = 0.1 m = 10 cm

4.4.5 Air Blowers

It is decided that we require only 2 air blowers for the process. Due to process air flow rate 1000 CFM with 8"WG air blower is bought from Canada Blower [Industrial Centrifugal Pumps Price Chart, 2013].

4.4.6 Water Pump

During the adsorption process, water level in the bubbler is stabilized by supplying water continuously. Required amount of water to increase the humidity of the flowing air to 100% relative humidity is calculated, and due to the flow rate range and common usage, Cole Parmer Magnetic Drive Centrifugal Pump is bought [Centrifugal Magnetic Drive Pumps, 2013].

4.4.7 Valves

Due to process' pipe diameter and low cost, 860-kPa rating carbon steel flanged valves are used. From process layout, it is shown that we need 10 valves for the plant [Peters et al., 2003].

4.4.8 Bubbler

Bubbler is designed by scaling up the current bubbler used in the experiments. This scale up is done by using residence time of the current bubbler, and volumetric flow rate of the process air in the plant. Scaling up calculations are explained in detail in Appendix 7.2.

Bubbler Volume = 5.01 m^3

Length (L) = Inside Diameter (D_i) = 1.85 m

Also, an ultrasonic fog generator is placed in the bubbler to ensure 100% relative humidity [Ocean Mist Industrial Ultrasonic Humidifier, 2013].

4.4.9 Water Trap

A water trap is required for the air exiting the bubbler. It captures the condensed water droplets to prevent the liquid from entering the adsorption column. As it has the same inlet and outlet flow rate as bubbler, a container with the same dimensions is used with an additional water exhaustion line.

Water Trap Volume = 5.01 m^3

4.5 Economic Analysis

4.5.1 Cost Estimation for 100 MWh/year Thermal Energy Storage Plant

After making a preliminary plant design, purchased equipment cost, total capital investment, and annual production cost are calculated. Then, by using these calculated values, thermal energy price is obtained for 15 years of payback period. All cost values are

calculated for the year of 2013. (Cost values are converted to this year by using inflation rates.)

4.5.1.1 Purchased Equipment Cost (PEC)

Purchased equipment cost is obtained by calculating the prices of each equipment separately. Costs of air filter, bubbler, water trap, heat exchanger, adsorption column, valves, and air blowers are added to obtain total purchased equipment cost value as shown in Table 4.3. Calculation of these cost values are explained in detail in Appendix 7.2.

Table 4.3: Purchased Equipment Cost for 100 MWh/year Energy Storage Plant

Equipment	**Price**
Air Filter	$375
Adsorption Column	$87,700
Heat Exchanger	$3,700
Air Blower (2)	$1,770
Water Pump	$870
Valves (10)	$2,480
Bubbler (Tank + Fog Generator)	$11,840
Water Trap	$10,540
Total PEC	**$119,275 ~ $119,300**

4.5.1.2 Total Capital Investment (TCI)

After the calculation of purchased equipment cost (PEC), total capital investment is estimated by using ratios of purchased equipment cost for a solid-fluid processing plant [Peters et al., 2003]. Total capital investment covers all of the plant installation costs such as purchased equipment installation, adsorbent cost, piping, electrical systems,

instrumentation and controls, buildings, service facilities, construction expenses, engineering and supervision, legal expenses, and etc. Detailed calculation total capital investment estimation for the 100 MWh/year thermal energy storage plant is shown in Table 4.4.

Table 4.4: Total Capital Investment Estimation (Solid-fluid Processing Plant) [Peters et al., 2003]

	Ratios	**Cost**
Direct Costs		
PEC Delivered	100	$119,300
Purchased-equipment Installation	39	$46,520
Adsorbent Cost	-	$150,000
Instrumentation and Controls	26	$31,020
Piping (installed)	31	$36,980
Electrical Systems (Installed)	10	$11,930
Buildings (including services)	29	$34,590
Yard improvements	12	$14,310
Service facilities (installed)	55	$65,610
Total direct plant cost	-	$510,260
Indirect Costs		
Engineering and supervision	32	$38,180
Construction expenses	34	$40,560
Legal expenses	4	$4,770
Contractor's fee	19	$22,670
Contingency	37	$44,140
Total indirect plant cost	126	$150,320
Total Capital Investment		

Fixed Capital (FCI) (Direct+Indirect)	-	$660,580
Working Capital (15% of TCI)	-	$116,570
Total Capital Investment	**503**	**$777,150**

4.5.1.3 Annual Production Cost

After estimating the installation cost of the whole thermal energy storage plant, yearly plant operation cost is calculated by using direct production costs (labor, utilities and etc.), fixed charges (depreciation and insurance), and general expenses (administrative, marketing and R&D costs). Ratios used in the calculation of annual production cost are directly taken from Peters & Timmerhaus [Peters et al., 2003]. Several cost values such as operating labor, utilities, and depreciation are calculated manually for the 100 MWh/year thermal energy storage plant. As almost all renewable energy plants are not paying taxes to the government, tax cost is neglected while calculating the annual production cost. Moreover, this plant is designed to be attached to a power plant in order to store its excess thermal energy, therefore, some cost values such as supervisory labor, rent, and marketing are neglected assuming that those costs will already be paid for the existing power plant. Calculation of the annual production cost is summarized in Table 4.5. Detailed calculation of manually estimated values (operating labor, utilities, and depreciation) are given in detail in Appendix 7.2.

Table 4.5: Estimation of annual production cost [Peters et al., 2003]

	Ratios	Cost
1. Manufacturing Cost		
A. Direct Production Costs		
Raw Materials	-	-
Operating Labor	-	$27,800
Direct Supervisory and Clerical Labor	-	-
Utilities	-	$2,815
Maintenance and Repairs	1% of Fixed Capital	$6,600
Operating Supplies	10% of Maintenance and Repairs	$660
Patents and Royalties	1% of Total Product Cost	$540
B. Fixed Charges		
Depreciation	-	$9,300
Local Taxes	-	-
Insurance	0.4% of Fixed Capital	$2,640
Rent	-	-
Financing	-	-
2. General Expenses		
Administrative Costs	10% of operating labor, and supervision	$2,780
Distribution and Marketing Costs	-	-
Research and Development Costs	-	-
Total Product Cost = Manufacturing Cost + General Expenses		
Total Product Cost	**-**	**53,650**

4.5.1.4 Thermal Energy Price

(a) Thermal Energy Price without Funding

Finally, a price for the stored thermal energy is estimated. Thermal energy price is calculated by assuming a payback period of 15 years for the 100 MWh/year thermal energy storage plant. Calculation is done by using total capital investment, annual production cost and payback period.

$$PaybackPeriod = \frac{TotalCapitalInvestment}{AnnualCapitalCost} \tag{4.2}$$

$$Total\ Cost = Annual\ Capital\ Cost + Total\ Product\ Cost \tag{4.3}$$

$$Thermal\ Energy\ Price = \frac{TotalCost(\$)}{YearlyEnergyStored(kWh)} \tag{4.4}$$

Thermal energy price for bare bone case is obtained by assuming that total capital investment is only composed of purchased equipment cost and the adsorbent cost. (Best case scenario).

Calculated thermal energy price values both for regular case and bare bone case are given in Table 4.6 as a summary.

Table 4.6: Thermal Energy Price without Funding

	100 MWh/year Storage	**100 MWh/year Storage (Bare Bone Case)**
Total Cost = Annual Production Cost + Annual Capital Cost		
Annual Capital Cost	$51,810	$17,950
Annual Production Cost	$53,650	$53,650
Total Cost	$105,460	$71,600
Energy Price = Total Cost/Total Energy Production		
Energy price/kWh	$1.055/kWh	$0.716/kWh

(b) Thermal Energy Price with Clean Energy Funding

Most of the governments in the world support clean and renewable energy plants by giving them a funding. For example, Canadian Government supports those plants through Clean Energy Funding. Therefore, a detailed comparison between the projects which already earned this funding is made and it is concluded that our thermal energy storage project will possibly earn a funding between $2.5 million to $5 million [Clean Energy Fund, 2012]. A funding amount of $2.5 million is assumed to be received for this plant. After assuming an average lifetime of the plant as 40 years (as it is the average lifetime of the building), yearly funding income is calculated as shown in equation 4.5.

$$\text{Yearly Funding Income} = \frac{TotalFunding}{AverageLifetime} = \frac{\$2.5\times10^{6}}{40\,years} = \$62{,}500/\,year \qquad (4.5)$$

Yearly funding income is deducted from the plant's yearly costs, and stored thermal energy price is calculated the same way as mentioned in section (a) for a payback period of 15 years. Calculation of thermal energy prices with the funding are given in Table 4.7.

Table 4.7: Thermal Energy Price with Clean Energy Funding

	100 MWh/year Storage	**100 MWh/year Storage (Bare Bone Case)**
Total Cost = Annual Production Cost + Annual Capital Cost		
Annual Capital Cost	$51,810	$17,950
Annual Production Cost	$53,650	$53,650
Yearly Funding Income	-$62,500	-$62,500
Total Cost	$42,960	$9,100
Energy Price = Total Cost/Total Energy Production		
Energy price/kWh	$0.462/kWh	$0.091/kWh

4.5.2 Cost Estimation for Different Storage Capacities

After obtaining purchased equipment cost, total capital investment, and annual production cost for 100 MWh/year thermal energy storage plant, same calculations are done for different storage capacities. Volumetric flow rate, dimensions of the purchased equipments and their costs, and amount of the Clean Energy Funding that is assumed to be received from Canadian Government are adjusted accordingly while estimating the cost values for the plants with different thermal energy storage capacities. Then, by using these calculated values, thermal energy price is obtained both for different thermal energy storage capacities and for different payback periods.

4.5.2.1 Purchased Equipment Cost (PEC)

Purchased equipment cost is obtained by calculating the price of each equipment separately for different thermal energy storage capacities. (Thus, for different air flow rates.)

Costs of air filter, bubbler, water trap, heat exchanger, adsorption column, valves, water pump, and air blowers are calculated separately for different energy storage capacities from 10 to 100 MWh/year. They are all added to obtain total purchased equipment cost value as shown in Figure 4.2.

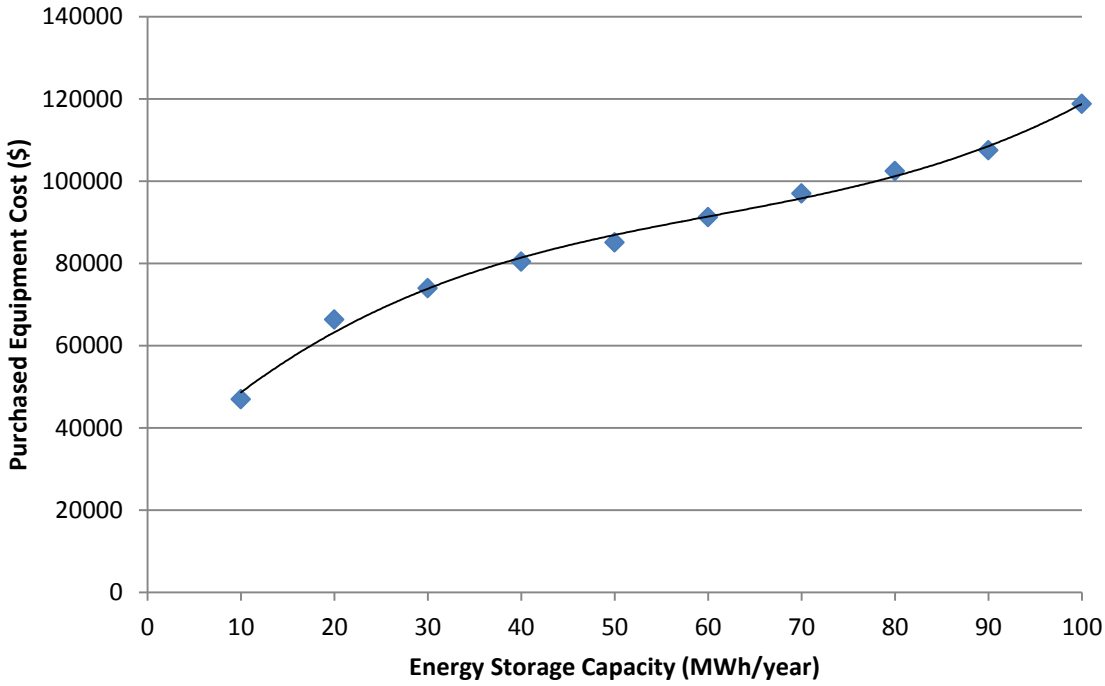

Figure 4.2: Purchased equipment cost with respect to the stored thermal energy

4.5.2.2 Total Capital Investment (TCI)

After the calculation of purchased equipment cost is done, total capital investment is estimated. This estimation is done by using the purchased equipment cost, and the ratios given in Table 4.4 for solid-fluid processing plants. While estimating total capital investment for the plants with different thermal energy storage capacities, adsorbent cost is adjusted for each plant. Calculated total capital investment values for different thermal energy storage capacities from 10 to 100 MWh/year are shown in Figure 4.3.

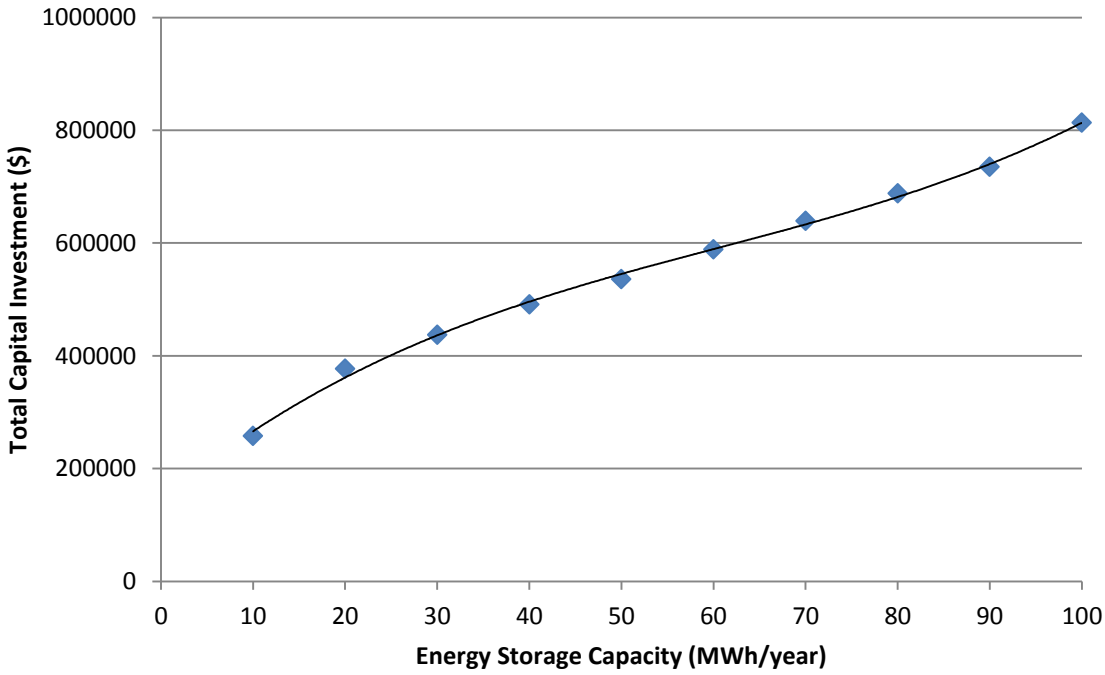

Figure 4.3: Total Capital investment with respect to stored thermal energy

4.5.2.3 Annual Production Cost

Annual production cost of the plants with different thermal energy storage capacities are calculated as explained in section 4.5.1.3. Calculations of the manually calculated cost items such as utilities and depreciation are adjusted for each plant with different thermal energy storage capacities. Annual production cost of the plants with respect to different thermal energy storage capacities are shown in Figure 4.4.

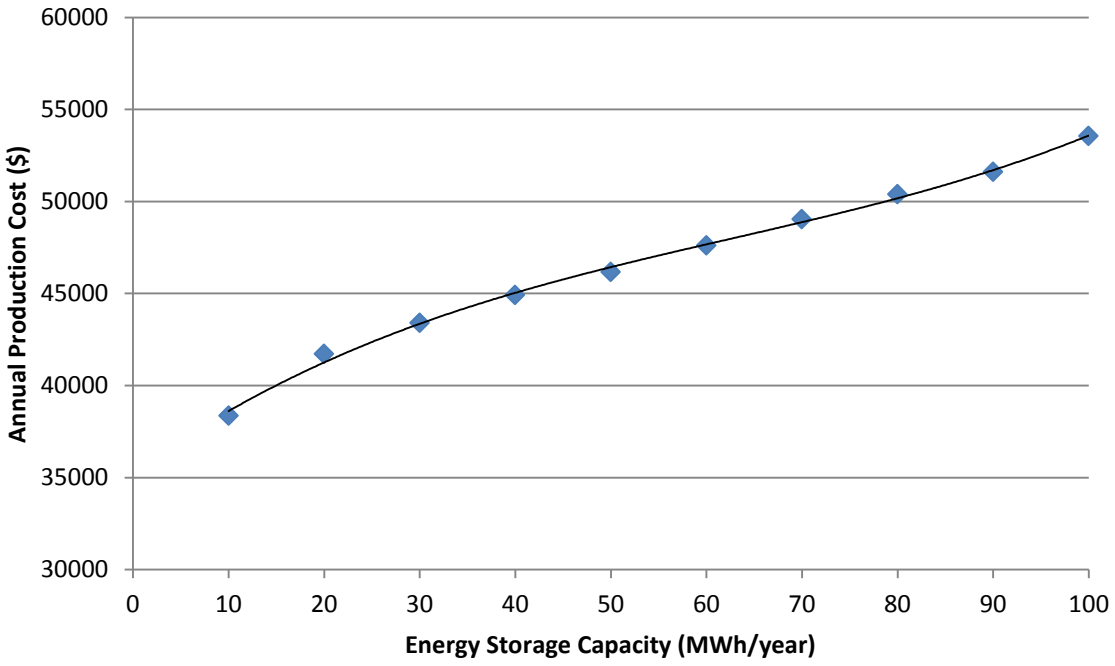

Figure 4.4: Annual production cost with respect to the stored thermal energy

4.5.2.4 Thermal Energy Price

(a) Thermal Energy Price without Funding

Thermal energy price is calculated for different energy storage capacities and for different payback periods as explained in section 4.5.1.4. This calculation is again done both for regular and bare bone cases. Thermal energy prices for regular and bare bone cases are given in figures 4.5 and 4.6, respectively.

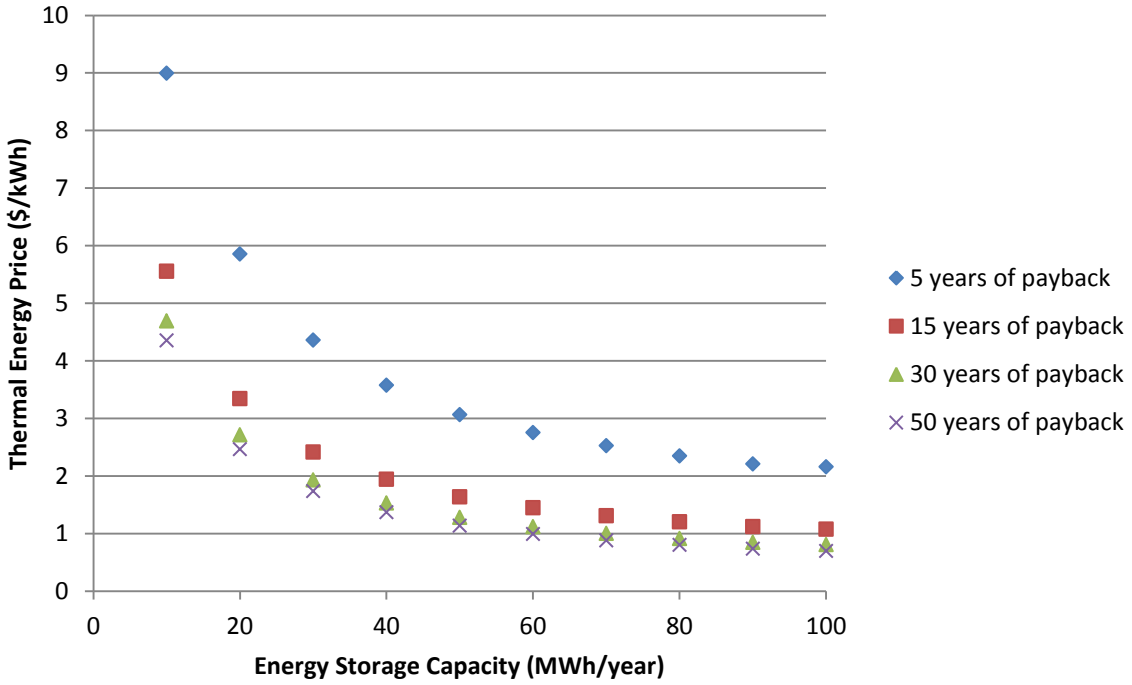

Figure 4.5: Thermal energy price for regular case with respect to stored energy for various payback periods for no clean energy funding.

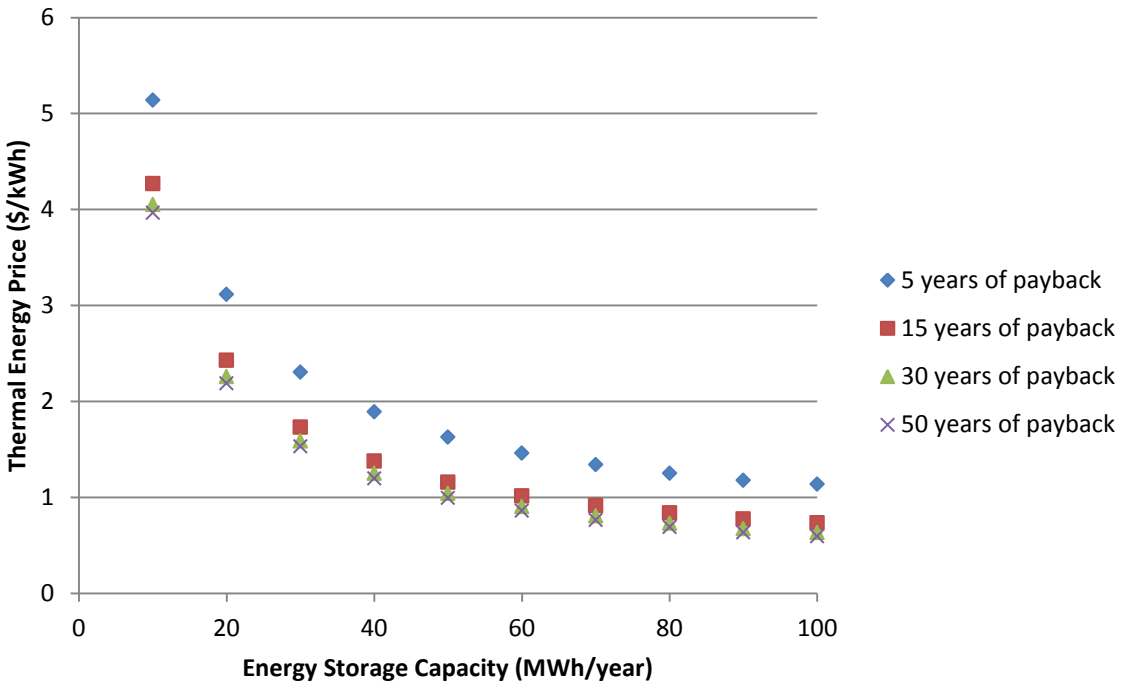

Figure 4.6: Thermal energy price for bare bone case with respect to stored energy for various payback periods for no clean energy funding.

(b) Thermal Energy Price with Clean Energy Funding

Before doing any further calculation, amount of Clean Energy Funding received from the Canadian Government is optimized for different thermal energy storage capacities. Then, thermal energy price is recalculated for each plant by using the purchased equipment cost, total capital investment, annual production cost, and amount of Clean Energy Funding received. This energy price calculation is done for different payback periods, and both for regular and bare bone cases. Estimated energy price values for regular and bare bone cases are shown in figures 4.7 and 4.8, respectively.

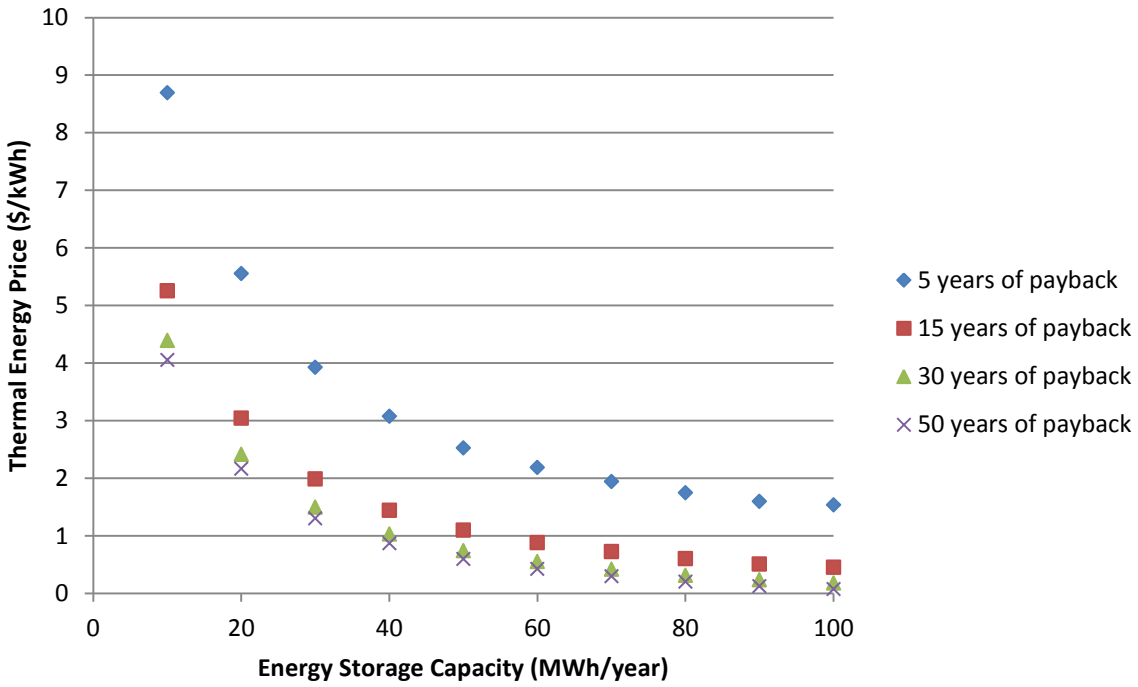

Figure 4.7: Thermal energy price for regular case with the clean energy funding with respect to the stored energy for various payback periods.

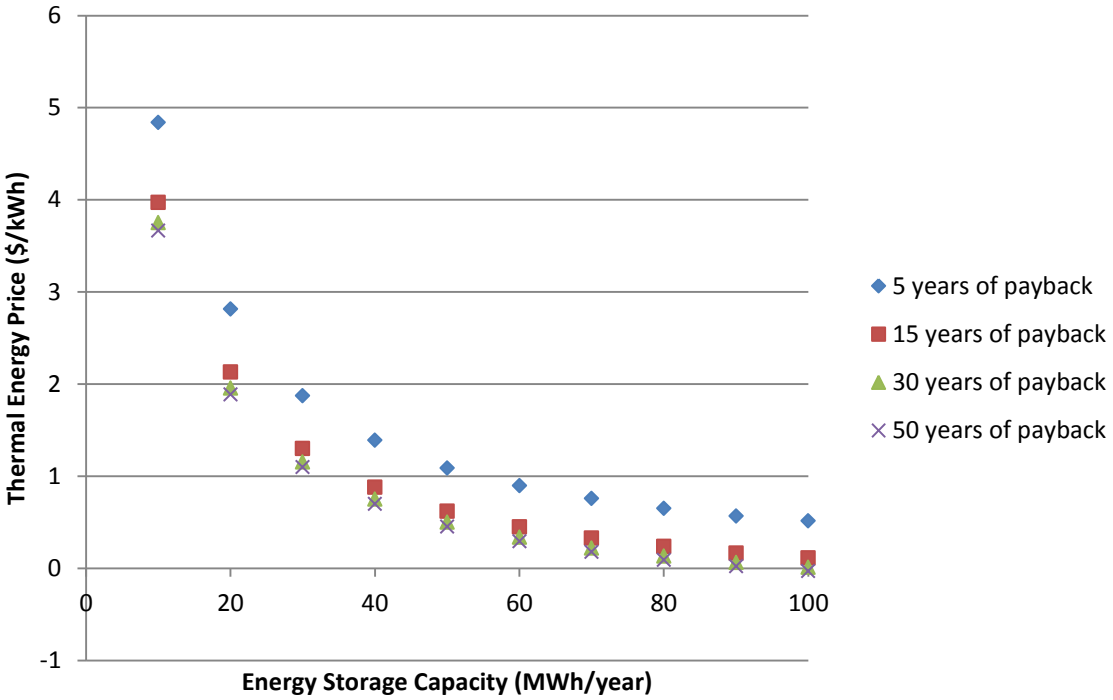

Figure 4.8: Thermal energy price for bare bone case with the clean energy funding with respect to the stored energy for various payback periods.

4.6 Discussions

In this chapter, plant design and economic analysis of thermal energy storage system in adsorbent beds are explained. One of the significant application areas of this system is storing the excess thermal energy supplied from power plants. In all power plants, after electricity production in turbine, exhaust gas which is around 400^{o}C goes through a heat exchanger for thermal energy production. However, almost one third of this produced thermal energy is excess and released to atmosphere [Waste Heat to Power Systems, 2013]. While conducting the plant design, in order to obtain more detailed and accurate cost estimations, thermal energy storage plant is designed to be attached to an existing power plant whose excess thermal energy will be stored.

Design and cost estimations of the several process equipments such as air filter, valves, pipes, air blowers, bubbler, and water trap are done by using the calculated volumetric flow rates for each plant at different thermal energy storage capacity per year.

Heat exchanger is used during desorption process of the thermal energy storage plant to heat the process air up to the regeneration temperature of 250^{o}C. Excess hot exhaust of the turbine in the power plant is used for this heating process. This heated air then passes through the adsorption column for complete regeneration. Shell-and-tube heat exchanger is decided to be used as a heat exchanger due to being economical. Dimensions of the heat exchanger are estimated by using the amount of energy required for complete regeneration of the adsorbent bed.

An adsorption column with a length/diameter ratio of 1 is used in the thermal energy storage plant in order to minimize the heat loss to the environment and to the adsorbents during the adsorption process. Carbon steel column is decided to be used as an adsorption column due to its low cost and wide temperature range. Insulation thickness is estimated by selecting a reasonable insulation thickness value in which heat loss from the column is minimized.

All equipment costs are added up to find total purchased equipment cost of the plant. Cost estimations of all equipments are done for the year of 2013. Equipment costs which are not provided for the year of 2013 are converted by using inflation rates. After calculating the purchased equipment cost, total capital investment cost required for the thermal energy storage plant is estimated. This estimation is done by using the ratios given for solid-fluid processing plants in Table 4.4 [Peters et al., 2003] and the amount of adsorbent required to fill the column. Total capital investment estimation is adjusted for each plant with different thermal energy storage capacities. Using ratios of purchased equipment cost gives out a rough estimation for total plant investment. This roughness can be eliminated by conducting a more detailed investment cost analysis for the plant.

Moreover, annual operation cost of the plant is estimated from manufacturing costs (labor, utilities, maintenance, rent, depreciation and etc.) and general expenses (administrative costs, marketing, research and development). Several cost items such as rent, marketing, research and development, and taxes are neglected as it assumed that they are already being paid for the existing power plant. Utilities and labor costs are calculated manually for

each plant at different thermal energy storage capacities, and for the calculation of the remaining cost items such as maintenance, patents and administrative costs, ratios of other cost values are used which are directly taken from Peters &Timmerhaus [Peters et al., 2003].

Finally, a thermal energy price for the stored thermal energy is estimated for each plant at different storage capacities and at different payback periods. This estimation is done for two cases: i) regular case (total capital investment is used as plant's investment), and ii) bare bone case (purchased equipment cost + adsorbent cost is used as plant's investment). Bare bone case is assumed to be the most cost effective case for a thermal energy storage plant which is attached to an existing power plant. For 100 MWh/year storage plant, thermal energy price is calculated as $1.055/kWh for the regular case and $0.716/kWh for the bare bone case with 15 years of payback period.

Furthermore, most of the clean energy plants are working with government support in all over the world. (They are supported especially in Canada with Clean Energy Funding [Clean Energy Fund, 2012].) Thus, assuming that our plant will also receive a funding, thermal energy price of the 100 MWh/year plant is estimated as $0.462/kWh for the regular case, and $0.091/kWh for the bare bone case. (This calculation is done for 15 years of payback period.) With the help of this funding, thermal energy price becomes lower than the electricity prices of many countries such as Tonga, Denmark, Germany, and Brazil. Electricity prices for some countries are shown in Table 4.8.

Table 4.8: Global electricity priknce comparison for 2012 [Electricity Pricing, 2012]

Country	Cents/kWh	Country	Cents/kWh
Tonga	57.95	Chile	23.11
Denmark	40.38	Singapore	22.83
Germany	36.48	UK	21.99
Brazil	34.18	Finland	20.65
Philippines	30.46	France	19.39
Belgium	29.06	New Zealand	19.15
Netherlands	28.89	China	16.00
Italy	28.39	Turkey	13.10
Ireland	28.36	Israel	12.34
Sweden	27.10	Hong Kong	12.04
Spain	27.06	USA	11.20
Portugal	25.25	Canada	10.78
Australia	25.00	Peru	10.44
Hungary	23.44	Russia	09.58

4.7 Conclusions

In this chapter, firstly, process of thermal energy storage in adsorbent beds is explained and its plant layout is shown. Then, the design of the pieces of the equipments used in the process is explained. Furthermore, total purchase equipment cost, total capital investment, and annual production cost are calculated for 100 MWh/year thermal energy storage capacity as a sample calculation. By assuming 15 years of payback period, thermal energy price is calculated for 100 MWh/year storage capacity for two cases: regular case, and bare bone case. Moreover, thermal energy price is recalculated for a case in which Clean Energy Funding from the government is received. Finally, this whole cost calculation and price estimation processes are done for different thermal energy storage capacities, and for different payback periods. During cost and price calculations for different plants at different energy storage capacities, all size, amount and cost estimations are adjusted accordingly.

4.8 References

Centrifugal Magnetic Drive Pumps. Retrieved on January 7, 2013 from http://www.coleparmer.com/Category/Centrifugal_Magnetic_Drive_Pumps_with_Enclosed_Motor_Flouroplastic/17268

Clean Energy Fund. Retrieved on April 17, 2012 from http://www.nrcan.gc.ca/media-room/news-release/01a/2010-01/1416

Dicaire, D. N., Tezel, H. F. (2011) "Regeneration and efficiency characterization of hybrid adsorbent for thermal energy storage of excess and solar heat". Renewable Energy, 36, 3, 986-992.

Duncan, R. (2009). "The City of Austin Energy Depletion Risks Task Force Report". Austin Energy, Texas, U.S.

Electricity Pricing (n.d.). In *Wikipedia.* Retrieved on February 22, 2013 from http://en.wikipedia.org/wiki/Electricity_pricing

HEPA Filters. Retrieved on February 9, 2013 from http://www.filt-air.com/Resources/Articles/hepa/hepa_filters.aspx

Industrial Centrifugal Fans Price Chart. Retrieved on February 16, 2013 from http://www.canadianblower.com/centrifugalfan/index.html

Naik-Dhungel, N. (2012). "Waste Heat to Power Systems". CHP &EPA Combined Heat and Power Partnership, U.S. Environmental Protection Agency.

Ocean Mist Industrial Ultrasonic Humidifier. Retrieved on January 20, 2013 from http://www.mainlandmart.com/humidify.html

Peters M., Timmerhaus K., West R. (2004). "Plant Design and Economics for Chemical Engineers". McGraw Hill, New York.

Vortec products price list 2008. Retrieved on January 20, 2013 from http://www.newmantools.com/price/vorprice.htm

Waste Heat to Power Systems, Retrieved on March 2, 2013 from http://www.epa.gov/chp/documents/waste_heat_power.pdf

5. Conclusions

Total energy produced is mostly consumed as thermal energy. Currently, more than 85% of thermal energy consumption is supplied from fossil fuels. This high rate of consumption increases the depletion risk of fossil fuels as well as causing a tremendous release of hazardous gases which affects both environment and human health. Those drawbacks lead humankind to search for new technologies, such as renewables, to produce thermal energy in order to reduce the dependency on fossil fuels.

Thermal energy storage in adsorbent beds is one of the resulting technologies. Adsorption is an exothermic process in which a fluid (adsorbate) diffuses into the pores of a porous solid (adsorbent), and is trapped into the crystal lattice. In adsorption thermal energy storage systems, either excess solar energy in summer months or excess thermal energy produced in power plants are stored in adsorbent beds by regeneration process. When thermal energy is required exothermic adsorption of water vapor from ambient air is carried out to heat processing air which can be used for space or water tank heating. In literature, the most efficient adsorbent for this process is found to be a hybrid adsorbent of activated alumina and zeolite.

In this report, after confirming literature data, a more efficient adsorbent which gives a higher energy density is searched. Then, feasibility of this system into large scale applications is proved. Moreover, applicability of on-off heat release for adsorption thermal energy storage systems is investigated. A model is established to describe exothermic adsorption process by doing mass and energy balances around the column, and

validity of this model is confirmed after comparing experimental and modeled results at different volumes and volumetric flow rates. Finally, an overall plant design and economic analysis of thermal energy storage plant are done for different storage capacities, and thermal energy prices are estimated.

As a conclusion, thermal energy storage system in adsorbent beds is a promising technology as it has a wide application range, feasible for different scales, easy to construct, and safe as only air and water are used in the process instead of various toxic compounds.

6. Acknowledgements

I would like to thank NSERC and Ottawa Technology Transfer Network for funding, and making it available to make a progress in this project. I would like to thank Dr. F. Handan Tezel for her precious guidance in my research, for her understanding throughout my studies, and for being there for me whenever I needed any kind of support. I would like to thank shop staff Louis, Gerard, and Franco for helping me in the laboratory. I would also like to thank Donatello, the Ninja Turtle, for increasing my interest in science when I was a little kid. I would like to thank my family for supporting and trusting me in my every decision, and especially my brother, Kemal Ugur, for being such an inspiring role model for me. Finally, I would like to thank Onur, my dear boyfriend, for making this whole Canada adventure priceless for me.

7. APPENDICES

7.1 Experimental Calculations

7.1.1 Humidity Equation Derivation

First of all, we need to derive an equation to obtain humidity of air (kg H_2O/kg dry air) from measured relative humidity values during the experiment. In order to obtain this equation, humidity values of 100% relative humidity (RH) air was read from psychometric chart at various temperatures [Perry and Green, 2008].

Table 7.1.1: Humidity with respect to temperature at 100% relative humidity

Humidity for 100 % RH		
Temp. (^oC)	**Humidity (kg H20/kg dry air)**	**Humidity (Fitted Data)**
15	0,0106	0,01079
16	0,0114	0,01149
17	0,0121	0,01223
18	0,013	0,01303
19	0,0139	0,01388
20	0,0149	0,01478
21	0,0158	0,01574
22	0,017	0,01676
23	0,018	0,01785
24	0,019	0,01901
25	0,0201	0,02024
26	0,0213	0,02155
27	0,0228	0,02295
28	0,0243	0,02444
29	0,026	0,02603
30	0,0274	0,02772

Then, those values are fitted and a trend line equation with the highest precision is obtained as shown below and equation 7.1 is obtained for 100% RH.

$$Humidity = 0.0042 \times e^{0.0629 \times T} \quad (7.1)$$

where Humidity = Air humidity [=] kg H_2O/kg dry air

Temp = Average temperature [=] ^oC

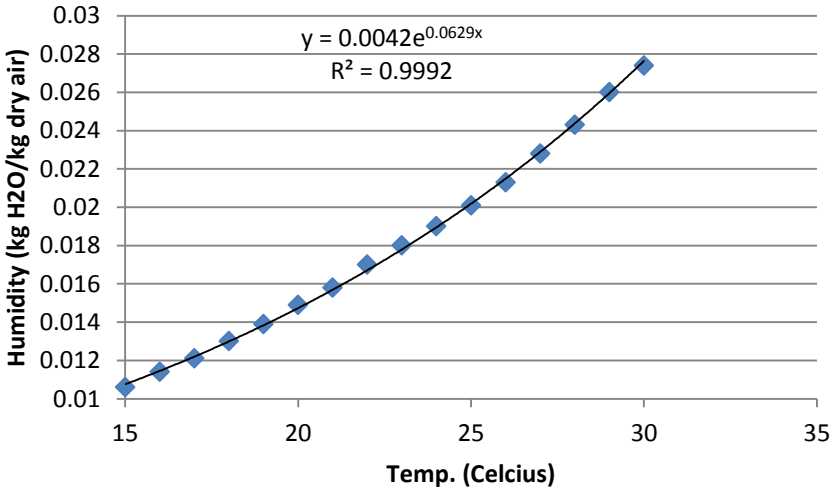

Figure 7.1.1: Air humidity with respect to average temperature at 100% relative humidity

Then, a relation between humidity and relative humidity was searched. In order to find this relation, humidity values at different relative humidities at the same temperature (20^oC) was read from psychometric chart. By observing the read values, we can conclude and fit this following relation (equation 7.2):

$$Humidity_{at\ x\%RH} = \left(\frac{x\%}{100}\right)(Humidity_{at100\%RH}) \quad (7.2)$$

Table 7.1.2: Humidity versus relative humidity

At 20°C		
RH (%)	**Humidity**	**Humidity (Fitted Data)**
100	0,0149	0,0149
90	0,0134	0,01341
80	0,0118	0,01192
70	0,0102	0,01043
60	0,0088	0,00894
50	0,0074	0,00745
40	0,006	0,00596
30	0,0044	0,00447
20	0,003	0,00298
10	0,0014	0,00149
0	0	0

By substituting equation 7.1 into equation 7.2, the final humidity calculation equation was obtained as equation 7.3:

$$Humidity = \left(\frac{x\%}{100}\right) \times 0.0042 \times e^{0.0629 \times T} \tag{7.3}$$

7.1.2 Moist Air Density Calculation

In order to calculate the moist air density, partial pressure of the water vapor is calculated by using equation 7.4 [Perry and Green, 2008].

$$p = \frac{P \times Y}{\left(\frac{M_v}{M_g}\right) + Y} \tag{7.4}$$

where p : water vapor pressure (Pa)

P: total pressure (Pa)

Y: humidity (kg H_2O/kg dry air)

M_v: water molecular weight (18.01 g/mol)

M_g: air molecular weight (28.97 g/mol)

After calculating water vapor partial pressure, it used to find moist air density from equation 7.5 [Perry and Green, 2008].

$$\rho_{air} = \frac{P - 0.378p}{287.1 \times T} \tag{7.5}$$

where ρ_{air} : moist air density (kg/m^3)

T : average temperature in the column (Kelvin)

7.1.3 Moist Air Heat Capacity Calculation

$C_s = C_{pg} + C_{pv}Y$ [Perry and Green, 2008] (7.6)

where C_s : moist air heat capacity (kJ/kg.K)

C_{pg} : dry air heat capacity (kJ/kg.K)

C_{pv} : water vapor heat capacity (kJ/kg.K)

Heat capacities of pure air and water vapor are calculated by using the equation 7.7 [Sandler, 2006].

$$C_p = (a + bT + cT^2 + dT^3)/MW \quad (7.7)$$

where C_p : heat capacity (kJ/kg.K)

T : average temperature in the column (Kelvin)

MW : molecular weight (g/mol)

For dry air: a = 28.088

b = 0.197×10^{-2}

c = 0.480×10^{-5}

d = -1.965×10^{-9}

MW = 28.97 g/mol

For water vapor: a = 32.218

b = 0.192×10^{-2}

c = 1.055×10^{-5}

d = -3.593×10^{-9}

MW = 28.97 g/mol

7.1.4 Energy Density Calculation

In order to calculate the energy density, total amount of moist air that flows through the whole process is found firstly.

Mass of moist air at each data point = $(t_i - t_{i-1})(Vol.Flow\ Rate)\left(\frac{1\ m^3}{1000\ L}\right)(\rho_{air,i})$ (7.8)

Total Mass of Moist Air = $\sum_{i=1}^{n}(t_i - t_{i-1})(Vol.Flow\ Rate)\left(\frac{1\ m^3}{1000\ L}\right)(\rho_{air,i})$ (7.9)

Then, C_{ps} is calculated at the average column temperature for every data point. Calculated C_{ps} and moist air mass values are used to find amount of energy released at each data point [Sandler, 2006].

Energy Released = (Moist Air Mass)(C_{ps})(T_{out} – T_{in}) (7.10)

Total Energy Released = $\sum_{i=1}^{n}(\text{Energy Released})$ (7.11)

where Vol. Flow Rate : set volumetric velocity during the experiment (L/min)

t : time in minutes

T_{out} : outlet column temperature

T_{in} : inlet column temperature

After calculating the total energy released, energy density is found as following equation 7.12.

$$Energy\ Density = \frac{Total\ Energy\ Released\ (kJ)}{Column\ Volume\ (m^3)} . \frac{1\ kWh}{3600\ kJ} \quad (7.12)$$

7.1.5 Adsorbent Capacity Calculation

In order to obtain adsorbent capacity, amount of water vapor adsorbed in each data point is calculated firstly [Perry and Green, 2008].

$$Dry\ Air\ Mass = \frac{Moist\ Air\ Mass}{(1+H_{out})} \quad (7.13)$$

$$H_2O\ Adsorbed = (Dry\ Air\ Mass)(H_{in} - H_{out}) \quad (7.14)$$

$$\text{Total } H_2O \text{ Adsorbed} = \sum_{i=1}^{n}(\mathrm{H_2O\ Adsorbed}) \quad (7.15)$$

$$Adsorbent\ Mass = (Volume) \times (Density) \quad (7.16)$$

$$Adsorbent\ Capacity = \frac{Total\ H_2O\ Adsorbed}{Adsorbent\ Mass} \quad (7.17)$$

where H_{out} = Outlet Humidity

H_{in} = Inlet Humidity

Adsorbent Density = 1061 kg/m^3

Volume = 62.76 mL = 6.276x10^{-5} m^3

7.1.6 Heat of Adsorption Calculation

Heat of adsorption is calculated experimentally by using equation 7.18.

$$Heat\ of\ Adsorption = \frac{Total\ Energy\ Released\ (kJ)}{(Total\ H_2O\ Adsorbed\ (kg)) \times \left(\frac{1000\frac{g}{kg}}{MW_{H2O}\frac{g}{mol}}\right)} \quad (7.18)$$

where Heat of Adsorption [=] kJ/mol

MW_{H2O} = 18.01 g/mol

7.2 Plant Design and Economic Analysis – Sample Calculations

7.2.1 Adsorption Column Design

a) Column Dimensions

Before starting the calculations, we assumed that energy density of the adsorption column is 200 kWh/m^3 as it is found in Chapter 2.

$$Working\ Volume = (100MWh) \times (\frac{1m^3}{200kWh}) \times (\frac{1000kWh}{1MWh}) = 500m^3 \quad (7.19)$$

In case of bubbling, outflow or expansion, a safety factor of 15% is used.

Total Volume = (500 m^3) (1.15) = 575 m^3

$V = \pi R_i^2 L = 575\ m^3$

For minimum cost and heat loss, inside diameter of the tank equals to its length. Therefore,

$L = D_i = 2R_i = 9.013$ m

b) Column Thickness

Before starting the calculations, we decided to use carbon steel column because of its low cost, resistance to high temperatures (during regeneration) and comparatively low thermal conductivity.

For a carbon steel cylindrical column, thickness of the column is found by equation 7.20 [Peters et al., 2003].

$$t = \frac{P.r_i}{S.E_j - 0.6P} + C_c \quad (7.20)$$

where t = thickness of the reactor

R_i = inside radius = 4.5065 m

C_c = allowence for corrosion = 0.0032 m (for carbon steel cylindrical reactor)

S = maximum allowable working stres = 94500 kPa (for carbon steel in the temperature range of -29 to 343 ^oC)

E_j = efficiency of joints expressed as a fraction = 0.6 (the minimum value is selected to account for the worst case scenario)

P = maximum allowable internal pressure = total bottom pressure

Total Bottom Pressure = Solid Pressure + Atmospheric Pressure

$$\text{Solid Pressure} = \frac{Weight}{Area} = \frac{V \times \rho \times g}{\pi \times R_i \times L} = \frac{(575m^3)(1061kg/m^3)(9.8m/s^2)}{\pi(4.5065m)(9.013m)} = 46854Pa \quad (7.21)$$

Atmospheric Pressure = 101.325 kPa

P = Total Bottom Pressure = 46.854 kPa + 101.325 kPa = 148.179 kPa

When those variables are substituted into the equation (7.20), column thickness is calculated as 15 mm as shown below.

$$t = \frac{(148.179\ kPa)(4.5065\ m)}{(94500kPa \times 0.6) - (0.6 \times 148.179kPa)} + 0.0032\ m = 0.015\ m = 15\ mm$$

c) Insulation Thickness

During the regeneration step (passing 250^{o}C hot through the column), high amounts of energy is given to the system. Therefore, insulation thickness is calculated in order to minimize the heat loss, thus the amount of energy given to the system during regeneration.

Heat loss equation for our cylindrical column during regeneration is given in equation 7.22 [Incropera et al., 2011].

$$Q = \frac{T_1 - T_4}{\frac{1}{(2\pi R_1 L)h_i} + \frac{\ln(R_2/R_1)}{2\pi L k_c} + \frac{\ln(R_3/R_2)}{2\pi L k_i} + \frac{1}{(2\pi R_3 L)h_o}} \quad (7.22)$$

where T_1 = temperature of the air inside the column = 250^{o}C

T_4 = temperature of ambient air = 20^{o}C

R_1 = inside radius of the column = (9.013/2) = 4.5065 m

R_2 = inside radius + thickness of the column = 4.5065 + 0.015 = 4.5215 m

L = length of the column = 9.013 m

h_i = heat transfer coefficient of the air inside the column

k_c = thermal conductivity of the column (carbon steel) = 36.3 W/m.K

k_i = thermal conductivity of cotton wool insulation = 0.029 W/m.K

R_3 = inside radius + thickness of the column + insulation thickness

h_o = heat transfer coefficent of the ambient air

Heat transfer coefficient of air flowing inside the column is calculated by using internal flow phenomena in circular tubes [Incropera et al., 2011]. Firstly, Reynolds number of the flowing air is calculated to determine the flow characteristics'.

$$\mathrm{Re} = \frac{\rho \upsilon D}{\mu} \tag{7.23}$$

where Re = Reynolds Number

ρ = 0.665 kg/m^3 = density of air at 250^{o}C

υ = superficial velocity = $\left(0.501\frac{m^3}{s}\right)\left(\frac{1}{\pi(4.5065m)^2}\right) = 0.00785\frac{m}{s}$

D = inside diameter of the column = 9.013 m

μ = 2.79x10^{-5} kg/m.s (viscosity of air at 250^{o}C)

$$\mathrm{Re} = \frac{\left(0.665\frac{kg}{m^3}\right)\left(0.00785\frac{m}{s}\right)(9.013m)}{2.79\cdot 10^{-5}\,\frac{kg}{m.s}} = 1686.4 < 2300 \Rightarrow \text{Laminar Flow}$$

As the Reynolds Number is smaller than 2300, the flow is laminar, and thus, Nusselt Number is equal to 3.66. Heat transfer coefficient of the internally flowing air is calculated by using the Nusselt Number and the equation 7.24 [Incropera et. al, 2011].

$$Nu = 3.66 = \frac{h_i D}{k} \tag{7.24}$$

where k = thermal conductivity of the air at 250°C = 0.0423 W/m.K

D = inside diameter of the column = 9.013 m

$$h_i = \frac{(3.66)\left(0.0423\frac{W}{m.K}\right)}{(9.013m)} = 0.017\frac{W}{m^2K}$$

Heat transfer coefficient of the air outside the column is calculated by using the free convection phenomena. Firstly, Rayleigh Number is calculated in order to determine the Nusselt Number of the system [Incropera et. al, 2011].

$$Ra_D = \frac{g\beta(T_s - T_\infty)L^3}{\nu\alpha} \tag{7.25}$$

where T_s = wall temperature = 230°C

T_∞ = ambient air temperature = 20°C

L = characteristic length of the column = 9.013 m

T_f = average temperature of the column wall and ambient air

$$= \frac{230 + 20}{2} + 273 = 398K \cong 400K$$

$\beta = 1/T_f = 0.0025\ K^{-1}$

ν = kinematic viscosity at T_f = $26.4 \cdot 10^{-6} m^2/s$

g = gravitational acceleration = 9.8 m/s^2

α = thermal diffusivity at T_f = $38.3 \cdot 10^{-6} m^2/s$

$$Ra_D = \frac{\left(9.8\frac{m}{s^2}\right)\left(0.0025K^{-1}\right)\left(230-20^oC\right)\left(9.013m\right)^3}{\left(26.4\cdot10^{-6}\frac{m^2}{s}\right)\left(38.3\cdot10^{-6}\frac{m^2}{s}\right)} = 3.72\cdot10^{11}$$

By using this calculated Rayleigh Number, Nusselt Number of the system is estimated, and heat transfer coefficient of the outside ambient air is calculated. Constants C and n in the equation 7.26 are estimated by using Rayleigh Number interval [Incropera et. al, 2011].

$$Nu_D = \frac{h_o D}{k} = C \cdot Ra_D^n \qquad (7.26)$$

where C = 0.125

n = 0.333

D = column diameter = 9.013 m

k = thermal conductivity of ambient air at T_f = 0.0338 W/m.K

h_o = 3.34 W/m^2K

Finally, by using these parameters, heat loss values are calculated for different R_3 values and a graph is plotted.

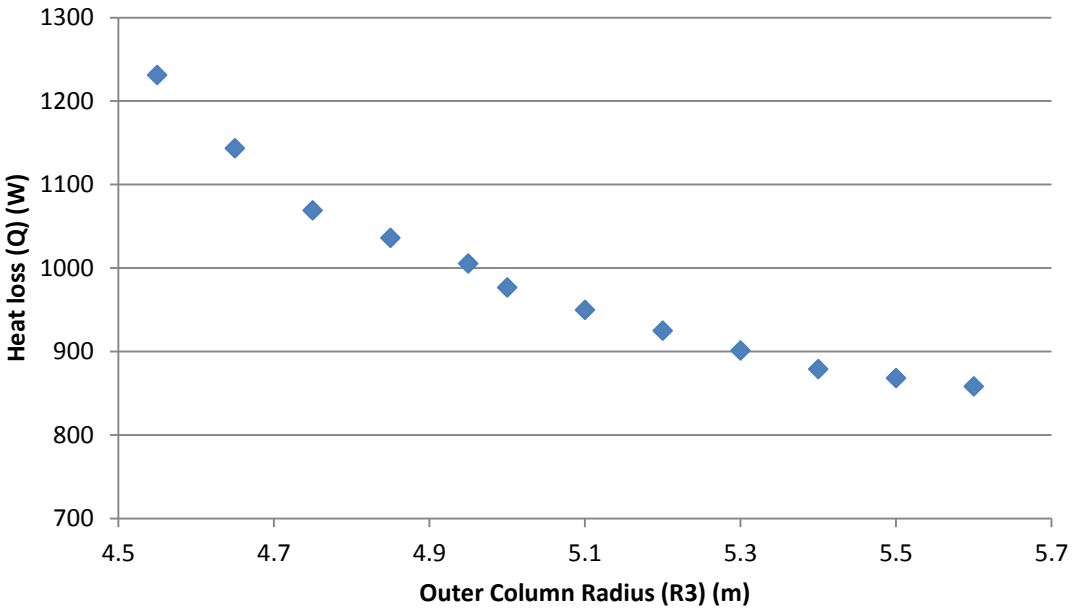

Figure 7.2.1: Amount of heat loss with respect to column diameter + insulation thickness

From this figure, a reasonable thickness value is selected to minimize the heat loss. R_3 is selected as 5.15 m. Thus, insulation thickness becomes 0.63 m.

Insulation Thickness = 0.63 m

d) Column Cost

<u>Tank:</u>

Column Volume = 575 m^3

From Fig 12-53 in Peters & Timmerhaus [Peters et al., 2003];

Purchase Cost = $40,000

From Fig 12-53, a cost correction factor of 1.75 is used due to the thickness of the column calculated in Appendix 7.2.1 part (b).

Corrected Purchase Cost = ($40,000)(1.75) = $70,000

As the cost estimations in Fig 12-53 is done for the year 2002, inflation rates between years 2002 and 2013 is used in order to estimate the tanks' 2013 price [Bank of Canada, 2013].

$$\frac{Cost\ Inflation\ Index\ of\ 2011-2012}{Cost\ Inflation\ Index\ of\ 2001-2002} = 1.24$$

Tank Purchase Cost = ($70,000)(1.24) = $86,800

Insulation: [Insulation, 2013]

$$Volume\ of\ Insulation = \pi R_o^2 L - \pi R^2 L = 172.53\ m^3$$

where R_o = outside radius = 5.15 m

R = inside radius + column thickness = 4.51987 m

L = 9.013 m

1 Parcel = (800x2400x100) mm = 0.192 m^3/$

Purchase Cost = $172.53\ m^3 . \frac{1\ \$}{0.192\ m^3} = \$\ 898.6 \sim \$900$

Total Purchase Cost = $86,800 + $900 = $87,700

7.2.2 Air Filter [Hepa Filters, 2013]

Air velocity = 0.501 m^3/s

HEPA Air Filter Dimensions = (610x610x149) mm

Area = (0.610 m)(0.610 m) = 0.3721 m^2

Air velocity = (0.501 m^3/s)/(0.3721 m^2) = 0.1864 m/s = 36.7 fpm

Purchase Cost = $375

7.2.3 Heat Exchanger

a) Amount of Heat Required for Desorption

From our adsorption experimental results, we know that air inside the column has an average temperature of 30^oC and an average relative humidity of 88.5%. Thus, by using a psychometric chart, partial pressure of water vapor in the air inside the column is found.

P_{H20} = 28.5 mm Hg = 3.8 kPa (partial pressure of water vapor at 30^oC and 88.5% RH)

By using the adsorption isotherm of water on activated alumina and zeolite, and partial pressure of water vapor, adsorption capacity is found as 13.0 mol H_2O/kg adsorbent.

$$Adsorbent\ Amount = (Volume)(density) = (575\ m^3)\left(1.144\frac{ton}{m^3}\right) = 657 \times 10^3\ kg$$

(7.27)

Amount of water adsorbed = (Adsorbent amount)(Adsorption capacity) (7.28)

= (657000 kg) (13.0 mol H_2O/kg) = 8541000 mol H_2O

Adsorption Energy = 42 kJ/mol H_2O (found experimentally in Chapter 2)

Total energy = (8541000 mol H_2O) (42 kJ/mol H_2O) (1 MWh/3.6x10^6) = 97.2 MWh (7.29)

So, 97.2 MWh energy is required to desorb water from adsorbent.

b) Heat Exchanger Cost

$$Q = 97.2 \frac{MWh}{year}$$

$$= \left(3.499 \times 10^8 \frac{kJ}{year}\right)\left(\frac{1\ year}{6\ months}\right)\left(\frac{1\ month}{30\ days}\right)\left(\frac{1\ day}{24\ h}\right)\left(\frac{1\ h}{3600\ s}\right) = 22.5\ kJ/s$$

$$= \left(22.5 \frac{kJ}{s}\right)\left(\frac{1\ BTU}{1.055056\ kJ}\right) = 21.325\ BTU/s$$

VOR.CC6360 Heat Exchanger is bought from ITW Vortec due to the amount of heat given from the heat exchanger [Vortec Price List 2008, 2013].

Price = $3,334.08

Following inflation rate is used in order to estimate the heat exchanger price for 2013 [Bank of Canada, 2013].

$$\frac{Cost\ Inflation\ Index\ of\ 2012 - 2013}{Cost\ Inflation\ Index\ of\ 2007 - 2008} = 1.09$$

Purchase Cost = ($3,334.08)(1.09) = $3,634 ~ $3,700

7.2.4 Air Blower

Air Flow Rate $= \left(0.501\ \frac{m^3}{s}\right)\left(\frac{1\ ft^3}{0.0283\ m^3}\right)\left(\frac{60\ s}{1\ min}\right) = 1052\ CFM$

1000 CFM with 10"WG air blower is bought from Canada Blower [Industrial Centrifugal Fans Price Chart, 2013]. One blower cost is $885 (for year 2013). In our system, there are 3 air blowers and their cost is calculated as below.

Purchase Cost = ($885) (2) = $1,770

7.2.5 Water Pump

Water is needed in bubbler to increase relative humidity to 100%.

Air flow rate = 0.501 m^3/s

At 20^oC, Humidity at 100% RH = 0.015 kg water vapor/kg dry air

$$\rho_{air} = \frac{P.MW}{RT} = \frac{(1atm)(29g/mol)}{(0.082\frac{L.atm}{K.mol})(293K)} = 1.207g/L = 1.207kg/m^3 \quad (7.30)$$

$Water\ vapor\ flow\ rate$

$$= (0.501m^3/s)(1.207kg/m^3)(0.015\frac{kgH_2O}{kgdryair})(\frac{3600s}{1h}) = 32.65kg/h$$

Due to the flow rate range and common usage, Cole Parmer Magnetic Drive Centrifugal Pump is bought [Centrifugal Magnetic Drive Pumps, 2013].

Purchase Cost = $870

7.2.6 Valves

Pipe Diameter = 10 cm = 0.1 m

From Fig. 12-7 in Peters & Timmerhaus [Peters et al., 2003];

Purchase Cost of 1 860-kPa rating carbon steel flanged valve = $200

In our plant, 10 valves are required.

Purchase Cost = (200$)x10 = $2000

Following inflation rate is used in order to calculate the price of valves for the year 2013 [Bank of Canada, 2013].

$$\frac{Cost\ Inflation\ Index\ of\ 2011-2012}{Cost\ Inflation\ Index\ of\ 2001-2002} = 1.24$$

Purchase Cost = ($2000)(1.24) = $2,480

7.2.7 Bubbler

Tank:

$$Residence\ time = \tau = \frac{Volume}{Volumetric\,Flow\,Rate} \tag{7.31}$$

$$\tau = \frac{4\ L}{26\ L/min} = 0.166\ \text{min} = 10\ s$$

$$Bubbler\ Volume = \left(0.501\frac{m^3}{s}\right)(10s) = 5.01 m^3$$

From Fig 12-53 [Peters et al., 2003];

Purchase Cost = 8500$

Purchase cost of the bubbler tank is adjusted for the year 2013 by using the following inflation rate [Bank of Canada, 2013].

$$\frac{Cost\ Inflation\ Index\ of\ 2011-2012}{Cost\ Inflation\ Index\ of\ 2001-2002} = 1.24$$

Purchase Cost = (8500$)*(1.24) = 10,540$

Ultrasonic Fog Generator:

$$Water\ vapor\ flow\ rate = (Air\ Flow\ rate)(Air\ density)(Humidity) \quad (7.32)$$

$$Water\ vapor\ flow\ rate$$

$$= \left(0.501\frac{m^3 humid\ air}{s}\right)\left(1.144\frac{kg\ humid\ air}{m^3\ humid\ air}\right)\left(0.014\frac{kg\ water\ vapor}{kg\ dry\ air}\right)$$

$$= 8.01 \times 10^{-3}\frac{kg\ water\ vapor}{s} = 28.8\ kg/h$$

Industrial Ultrasonic humidifier is selected and bought from MainlandMart.com due to the water flow rate in the process [Ocean Mist Industrial Humidifier, 2013].

Purchase Cost of Fog Generator = $1,298

Total Purchase Cost = $10,540 + $1,298 ~ $11,840

7.2.8 Water Trap

A water trap is required for the air exiting the bubbler. It captures the water which condenses from the vapor to prevent the liquid from entering the adsorption column. It is basically a container so that entering humid air can leave the condensed water droplets. As it has the same inlet and outlet flow rate as bubbler, a container with the same dimensions is used with an additional water exhaustion line.

Water Trap Volume = 5.01 m^3

Length (L) = Inside Diameter (D_i) = 1.85 m

From Fig 12-53 [Peters et al., 2003];

Purchase Cost = 8500$

Purchase cost of the bubbler tank is adjusted for the year 2013 by using the following inflation rate [Bank of Canada, 2013].

$$\frac{Cost\ Inflation\ Index\ of\ 2011-2012}{Cost\ Inflation\ Index\ of\ 2001-2002} = 1.24$$

Purchase Cost = (8500$)*(1.24) = 10,540$

7.2.9 Operating Labor

In addition to wages of labors, their insurance also have a considerable cost to plant. Monthly cost of labors to plant is calculated as shown in equation 7.32 [Peters et al., 2003].

Cost to company of a labor = net wage + tax + social security + others

$$= \text{net wage} \times 1.3 \tag{7.33}$$

Number of Labors:

Number of labors (workers) per shift is calculated from the Table 6.13 in Peters & Timmerhaus [Peters et al., 2003]. From the process layout, it can be found that we have 1 process vessels (bubbler and adsorption column), and 1 heat exchanger (shell & tube).

Process Vessels = 0.5x (2 process vessel) = 1.0 worker/day (7.34)

Heat exchanger = 0.1x (1 heat exchanger) = 0.1 worker/day (7.35)

Total workers = 1.0 + 0.1 = 1.1 ~ 1 worker/day (7.36)

Cost of Labors:

Net wage/labor= $10.25/h (minimum wage for Canada) [Hourly Minimum Wages in Canada for Adult Workers, 2013].

Cost to Company/labor = ($10.25/h)x1.3 = $13.325/h

Total cost to company = $\left(\frac{\$13.325}{h.wor\,\mathrm{ker}}\right)(1wor\,\mathrm{ker})\left(\frac{8h}{1day}\right)\left(\frac{5day}{1week}\right)\left(\frac{52week}{1year}\right) \cong \$27{,}800/year$

7.2.10 Utilities

a) Electricity

From Air Blowers: [Industrial Centifugal Fans Price Chart, 2013]

Air blowers bought from Canada Blower works with a power of 3 HP which is equal to 2240 W. (1 HP = 745.7 Watts)

$$W = \left(2240\frac{J}{s}\right)\left(\frac{24\ h}{1\ day}\right)\left(\frac{30\ day}{1\ month}\right)\left(\frac{12\ month}{1\ year}\right)\left(\frac{1}{2}\right) = 9.68\ MWh/year$$

In our plant, there are 3 air blowers. Thus total power consumption becomes

W_o = (9.68 MWh/year) (3) = 29.1 MWh/year

From Ultrasonic Fog Generator: [Ocean Mist Industrial Ultrasonic Humidifier, 2013]

MHS6 is bought from ITW Vortec with power of 700 W

$$W = \left(700\frac{J}{s}\right)\left(\frac{24h}{1day}\right)\left(\frac{30day}{1month}\right)\left(\frac{12month}{1year}\right)\left(\frac{1}{2}\right) = 3.03MWh/\ year \quad (7.37)$$

Total Electricity Consumption = 29.1 + 3.03 = 32.13 MWh/year

Electricity Cost:

Electricity price for Ottawa = $0.071/kWh [Electricity Rates & Conditions, 2013]

Electricity cost = ($0.071/kWh)(32.13 MWh/year)(1000 kWh/1 MWh)~$2,290/year

b) Water

Amount of water that is bought = 32.65 kg/h = 282.1 m^3/year (calculated in section 7.2.5)

Water price for Ottawa = $1.8534/$m^3$ [Water and Sewer Bills, 2013]

Water Cost = ($1.8534/$m^3$)(282.1 m^3/year) = $525/year

c) Total Utility Cost (Electricity + Water)

Total Utility = $2,290/year + 525/year = $2,815/year

7.2.11 Depreciation

Depreciation is calculated by using the following equipment life values and calculated cost values for those equipments. [General Guidelines for Depreciable Life, 2013]

100 MWh Storage:

Building ($30,770): 40 years

Machinery & Equipment ($106,100): 20 years

Piping ($32,890): 15 years

$$Depreciation = \frac{\$34{,}590}{40\,years} + \frac{\$119{,}300}{20\,years} + \frac{\$36{,}980}{15\,years} \cong \$9{,}300\,/\,year \quad (7.38)$$

7.3 References

Bank of Canada: Inflation Calculator. Retrieved on February 9, 2013 from http://www.bankofcanada.ca/rates/related/inflation-calculator/

Centrifugal Magnetic Drive Pumps. Retrieved on January 7, 2013 from http://www.coleparmer.com/Category/Centrifugal_Magnetic_Drive_Pumps_with_Enclosed_Motor_Flouroplastic/17268

Electricity Rates & Conditions. Retrieved on February 20, 2013 from http://www.hydroottawa.com/residential/index.cfm?lang=e&template_id=118

General Guidelines for Depreciable Life. Retrieved on February 22, 2013 from http://finance.duke.edu/accounting/gap/m200-090.php

HEPA Filters. Retrieved on February 9, 2013 from http://www.filt-air.com/Resources/Articles/hepa/hepa_filters.aspx

Hourly Minimum Wages in Canada for Adult Workers. Retrieved on February 26, 2013 from http://srv116.services.gc.ca/dimt-wid/sm-mw/rpt2.aspx?lang=eng&dec=5

Incropera, F. P., David, P. D., Bergman, T. L., Lavine, A. S. (2011) “Introduction to Heat Transfer”. John Wiley & Sons, New Jersey.

Industrial Centrifugal Fans Price Chart. Retrieved on February 16, 2013 from http://www.canadianblower.com/centrifugalfan/index.html

Insulation cotton. Retrieved on January 11, 2013 from http://www.alibaba.com/product-gs/429191192/Insulation_cotton.html

Ocean Mist Industrial Ultrasonic Humidifier. Retrieved on January 20, 2013 from http://www.mainlandmart.com/humidify.html

Perry, R. H., Green, D. W. 'Perry's Chemical Engineers' Handbook". McGraw Hill, New York, 2008.

Peters M., Timmerhaus K., West R. (2004). "Plant Design and Economics for Chemical Engineers". McGraw Hill, New York.

Sandler, S.I. "Chemical, Biochemical, and Engineering Thermodynamics", 4th Ed., John Wiley & Sons, New York, 2006.

Vortec products price list 2008. Retrieved on January 20, 2013 from http://www.newmantools.com/price/vorprice.htm

Water and Sewer Bills. Retrieved on February 20, 2013 from http://ottawa.ca/en/residents/ water-and-environment/water-and-sewer-bills/changes-your-water-and-sewer-bill

THIS PAGE LEFT BLANK INTENTIONALLY